metals

MDPI

Review

A Review of Recent Advances in Depression Techniques for Flotation Separation of Cu–Mo Sulfides in Porphyry Copper Deposits

Ilhwan Park [1,*], Seunggwan Hong [2], Sanghee Jeon [1], Mayumi Ito [1] and Naoki Hiroyoshi [1]

1 Division of Sustainable Resources Engineering, Faculty of Engineering, Hokkaido University, Sapporo 060-8628, Japan; shjun1121@eng.hokudai.ac.jp (S.J.); itomayu@eng.hokudai.ac.jp (M.I.); hiroyosi@eng.hokudai.ac.jp (N.H.)

2 Division of Sustainable Resources Engineering, Graduate School of Engineering, Hokkaido University, Sapporo 060-8628, Japan; chanitroi@gmail.com

* Correspondence: i-park@eng.hokudai.ac.jp; Tel.: +81-11-706-6315

Received: 29 August 2020; Accepted: 16 September 2020; Published: 21 September 2020

Abstract: Porphyry copper deposits (PCDs) are some of the most important sources of copper (Cu) and molybdenum (Mo). Typically, the separation and recovery of chalcopyrite ($CuFeS_2$) and molybdenite (MoS_2), the major Cu and Mo minerals, respectively, in PCDs are achieved by two-step flotation involving (1) bulk flotation to separate Cu–Mo concentrates and tailings (e.g., pyrite, silicate, and aluminosilicate minerals) and (2) Cu–Mo flotation to separate chalcopyrite and molybdenite. In Cu–Mo flotation, chalcopyrite is depressed using Cu depressants, such as NaHS, Na_2S, Nokes reagent (P_2S_5 + NaOH), and NaCN, meaning that it is recovered as tailings, while molybdenite is floated and recovered as froth product. Although conventionally used depressants are effective in the separation of Cu and Mo, they have the potential to emit toxic and deadly gases such as H_2S and HCN when operating conditions are not properly controlled. To address these problems caused by the use of conventional depressants, many studies aimed to develop alternative methods of depressing either chalcopyrite or molybdenite. In this review, recent advances in chalcopyrite and molybdenite depressions for Cu–Mo flotation separation are reviewed, including alternative organic and inorganic depressants for Cu or Mo, as well as oxidation-treatment technologies, such as ozone (O_3), plasma, hydrogen peroxide (H_2O_2), and electrolysis, which create hydrophilic coatings on the mineral surface.

Keywords: porphyry copper deposits; chalcopyrite; molybdenite; flotation; conventional and alternative depression techniques

1. Introduction

Porphyry copper deposits (PCDs) are the world's most important sources of copper (Cu) because they account for more than 60% of global annual copper production [1,2]. Although these deposits are widespread, they seem to be localized in time and space within the overall evolutionary pattern of magmatic arcs along plate convergent margins; that is, they are predominantly associated with (i) Mesozoic to Cenozoic orogenic belts in western North and South America, (ii) Tethyan orogenic belts in eastern Europe and southern Asia, and (iii) Paleozoic orogens in Central Asia and eastern North America (Figure 1) [1,3–5]. PCDs are low-grade (around 0.3–2.0% Cu; average 0.44% copper in 2008); however, they have significant economic value due to their large size (typically greater than 100 million tons), long mine lives (spanning several decades), and high production rates (i.e., millions of tons of copper per year) [1]. These deposits are also important sources of molybdenum (Mo), gold (Au), and silver (Ag) [1,5]. PCDs greatly contribute to the world's supply of Mo, accounting for more than 50% of the total supply [6]. In addition, elevated concentrations of rhenium (Re),

tellurium (Te), and platinum-group elements (PGEs) are incorporated in PCDs, which are recovered as byproducts; that is, Re, Te, and PGEs are mostly recovered from processes related to molybdenite (MoS_2), anode slimes generated from the electrorefining of copper anodes, and the smelting of copper ores, respectively [1].

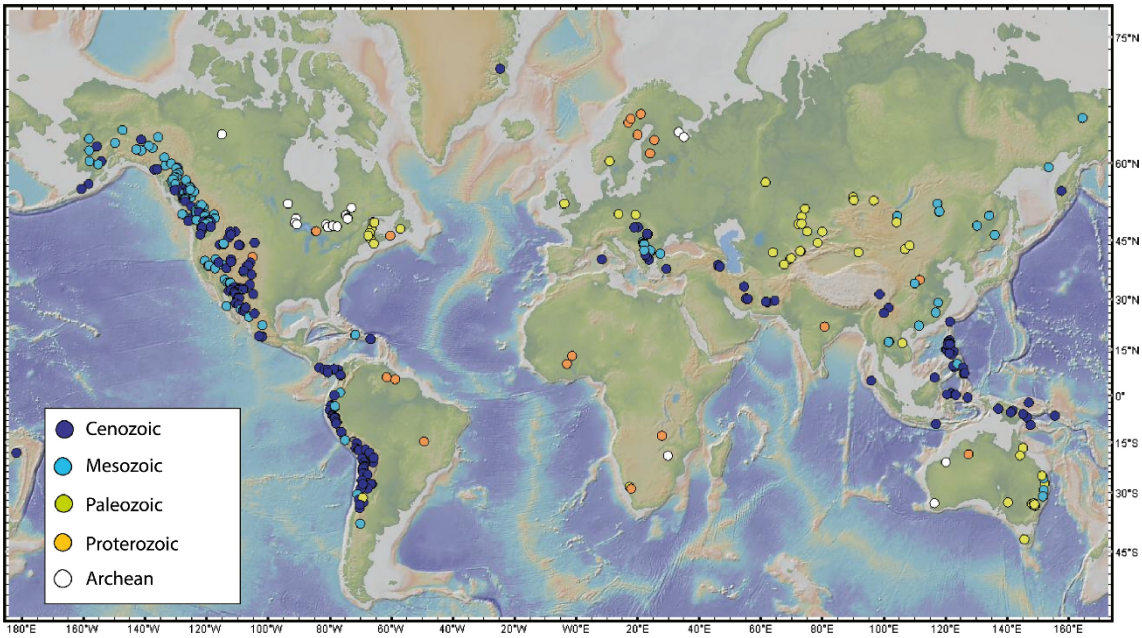

Figure 1. Occurrence of porphyry copper deposits through time (reprinted with permission from Lee and Tang [3], copyright (2020) Elsevier).

Typically, the recovery of copper sulfides (mostly chalcopyrite) and molybdenite from PCDs is conducted via a series of processes; that is, open-pit mining of PCDs to excavate the ores, closed-circuit comminution to liberate valuable and nonvaluable minerals, and multistep flotation of ground ores to separate Cu–Mo concentrates and tailings (e.g., pyrite and silicate minerals), followed by the separation of Cu and Mo minerals from Cu–Mo concentrates by flotation using Cu depressants (e.g., NaHS, Na_2S, Nokes reagent (P_2S_5 + NaOH), and NaCN)—the detailed processes for PCDs are discussed in the following section. Afterwards, Cu concentrates are treated by a pyrometallurgical process to produce Cu metal, while Mo concentrates are treated by leaching using HCl–$FeCl_3$ to produce the high-grade MoS_2 used for lubricants, or by roasting and acid pressure-oxidation processes to produce technical Mo oxide (MoO_3) [7].

During Cu–Mo flotation separation, Cu depressants work effectively to separate Cu and Mo minerals, but there are serious drawbacks, such as (i) the potential to release toxic and deadly gases (e.g., H_2S and HCN) when pulp pH is not properly maintained; (ii) the corrosive nature of Cu depressants, which destroy pipelines; (iii) the imperfect recovery of molybdenite; and (iv) considerable losses of precious metals such as gold and silver when cyanide is used [8–10]. In order to replace conventionally used Cu depressants, which have the above limitations, many studies have been conducted to develop alternative methods, including the use of environmentally friendly organic and inorganic depressants to reduce the floatability of either chalcopyrite or molybdenite, and oxidation treatments involving the use of ozone (O_3), plasma, hydrogen peroxide (H_2O_2), and electrolysis to create hydrophilic coatings on the surfaces of the chalcopyrite. Despite the existence of extensive studies, there is no review that summarizes all findings on this important topic. In this review, therefore, newly developed techniques for Cu–Mo flotation separation are reviewed. Specifically, we discuss mechanisms involved in selective depression for either chalcopyrite or molybdenite, and the advantages and disadvantages of each technique.

2. Typical Process of Cu–Mo Sulfide Ores

Figure 2 shows the typical flow sheet for the beneficiation of Cu–Mo sulfide ores, consisting of three steps: (1) comminution to liberate target minerals, (2) bulk flotation to recover Cu–Mo minerals from gangue minerals, and (3) selective flotation of Mo minerals (mostly molybdenite) from Cu–Mo bulk concentrates [10]. The ores are first crushed by a primary crusher, such as a jaw or gyratory crusher, and then ground with a semi-autogenous (SAG) and/or ball mill where conditioning agents such as a Cu–Mo collector (e.g., xanthate- and/or oil-based collector(s)) and pH adjuster (e.g., lime (CaO)) are introduced to improve the separation of Cu–Mo and gangue minerals during bulk flotation. The purpose of adding lime is to make the pulp pH alkaline, at which pyrite, one of the representative gangue minerals, could be effectively depressed. This depression of pyrite under alkaline conditions could be explained by the competitive adsorption of OH^- and the xanthate-based collector. There are critical pH values for sulfide minerals, below which xanthate ion can be adsorbed, while above which its adsorption is inhibited due to the competitive adsorption of OH^- [11]. For instance, critical pH values for pyrite and chalcopyrite in the solution containing 25 mg/L potassium ethyl xanthate at room temperature are 10.5 and 11.8, respectively, so the selective flotation of chalcopyrite could be achieved when pulp pH is adjusted to be between 10.5 and 11.8 [11]. There are two additional mechanisms of pyrite depression under alkaline conditions: (i) dixanthogen, an adsorbed form of xanthate-based collector on pyrite surface, becomes thermodynamically unstable; and (ii) pyrite surface is covered with ferric hydroxide having a hydrophilic nature [12]. After bulk flotation, tailings are disposed of into the tailings storage facility (TSF), while concentrates are transferred to the conditioning process, followed by flotation for the separation of Cu and Mo minerals. As shown in Figure 2, the conditioning process is aimed at depressing Cu minerals by using Cu depressants such as NaHS. This depressant is readily dissociated in the aqueous solution, and produces NaOH and H_2S (Equation (1)). At pH 9–10, H_2S is transformed into HS^- (Equation (2)), which reacts with xanthate-adsorbed Cu minerals; thereby, the surfaces of Cu minerals are modified from hydrophobic to hydrophilic due to the desorption of xanthate adsorbed on them (Equation (3), where CuX denotes the surface of xanthate-adsorbed Cu minerals). After pretreating Cu–Mo bulk concentrates with NaHS, Mo minerals are recovered as froth products, while Cu minerals are recovered as tailings. According to Hirajima et al. [13], the pretreatment of Cu–Mo bulk concentrates using NaHS significantly decreased Cu recovery from 85 to 10%, while Mo recovery was increased from 85 to 99% (Figure 3), indicating that NaHS was effective in selectively depressing Cu minerals. As a result of a single stage of Cu–Mo flotation using NaHS, the froth product contains around 10% Cu, which is most likely caused by entrainment. In industry, thus, froth products are further processed via multiple cleaning stages to meet the requirement of saleable Mo concentrates.

$$NaHS + H_2O \leftrightarrow NaOH + H_2S \tag{1}$$

$$H_2S \leftrightarrow H^+ + HS^- \tag{2}$$

$$2CuX + HS^- \leftrightarrow Cu_2S + 2X^- + H^+ \tag{3}$$

Similarly, the Nokes reagent (P_2S_5 + NaOH), Na_2S, and NaCN were also adopted as Cu depressants [7,10,14,15]. The function of the Nokes reagent and Na_2S is the same as that of NaHS for producing HS^-, which desorbs the adsorbed xanthate on Cu minerals (Equations (2)–(6)).

$$P_2S_5 + 6NaOH \leftrightarrow 2Na_3PO_2S_2 + H_2S + 2H_2O \tag{4}$$

$$P_2S_5 + 10NaOH \leftrightarrow Na_3PO_2S_2 + Na_3PO_3S + 2Na_2S + 5H_2O \tag{5}$$

$$Na_2S + 2H_2O \leftrightarrow H_2S + 2NaOH \tag{6}$$

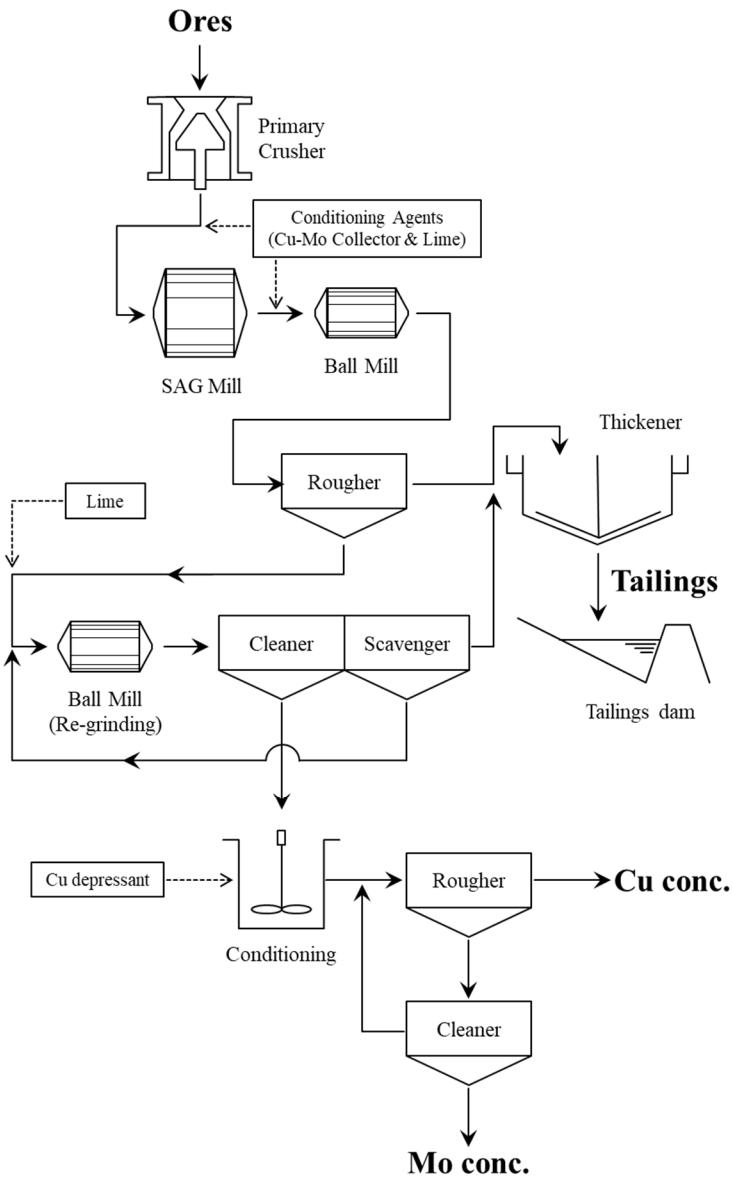

Figure 2. Beneficiation flowsheet of Cu–Mo sulfide ores [7].

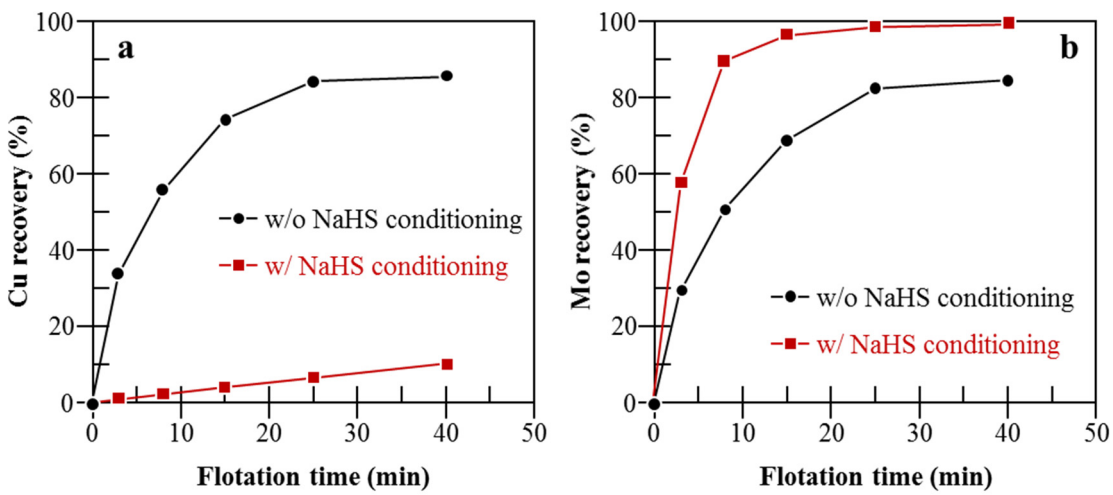

Figure 3. Effects of NaHS on recovery of (**a**) chalcopyrite and (**b**) molybdenite (reprinted with permission from Hirajima et al. [13], copyright (2017) Elsevier).

In the case of NaCN, its depressive mechanism is different, as NaCN is hydrolyzed in aqueous solution to form NaOH and HCN (Equation (7)). Then, the latter dissociates to CN^- under alkaline conditions (Equation (8)). The action of CN^- as a Cu depressant lies in its strong ability to form a copper–cyanide complex (Equation (9)) [14].

$$NaCN + H_2O \leftrightarrow NaOH + HCN \tag{7}$$

$$HCN \leftrightarrow H^+ + CN^- \tag{8}$$

$$2Cu^{2+} + 6CN^- \leftrightarrow 2[Cu(CN)_2]^- + C_2N_2 \tag{9}$$

By increasing the concentration of CN^-, it creates additional species of the copper–cyanide complex such as $[Cu(CN)_3]^{2-}$ and $[Cu(CN)_4]^{3-}$ [16]. Cyanide reacts with not only Cu^{2+}, but also copper–xanthate formed on the surfaces of Cu minerals, resulting in a decrease in their hydrophobicity due to the replacement of xanthate with cyanide. In addition, cyanide can directly react with the surface of Cu minerals where CN^- is adsorbed, thereby making it impossible to adsorb xanthate [16], and it is a reducing agent that reduces pulp potential in which chalcopyrite does not float.

Although effective, these depressants typically used for Cu–Mo separation have the potential to generate toxic and lethal gases if used haphazardly. As shown in Figure 4, the protonated forms of H_2S and HCN start forming at a pH below 10 and 12, respectively. Once they exist in aqueous solution, their vaporizations are readily progressed even under ambient conditions due to their relatively high vapor pressure (i.e., P_{H2S} = 20.03 atm at 25 °C; P_{HCN} = 0.98 atm at 25 °C) [17,18]. The problem of the formation of vaporized H_2S and HCN lies in its serious toxicity to human beings, the toxic actions of which occur via the inhibition of cytochrome oxidase that prevents the cellular utilization of oxygen, followed by the inhibition of the terminal step of electron transport in brain cells, resulting in loss of consciousness, respiratory arrest, and ultimately death [19,20]. Another problem of using NaCN in flotation is the significant losses of precious metals such as gold and silver incorporated in PCDs because cyanide is known to dissolve them by forming stable complexes [10]. Because of these problems, mineral-processing plants in which conventional depressants are used should either consist of covered flotation cells with an active ventilation system or always maintain pulp pH at above around 9.5 [21].

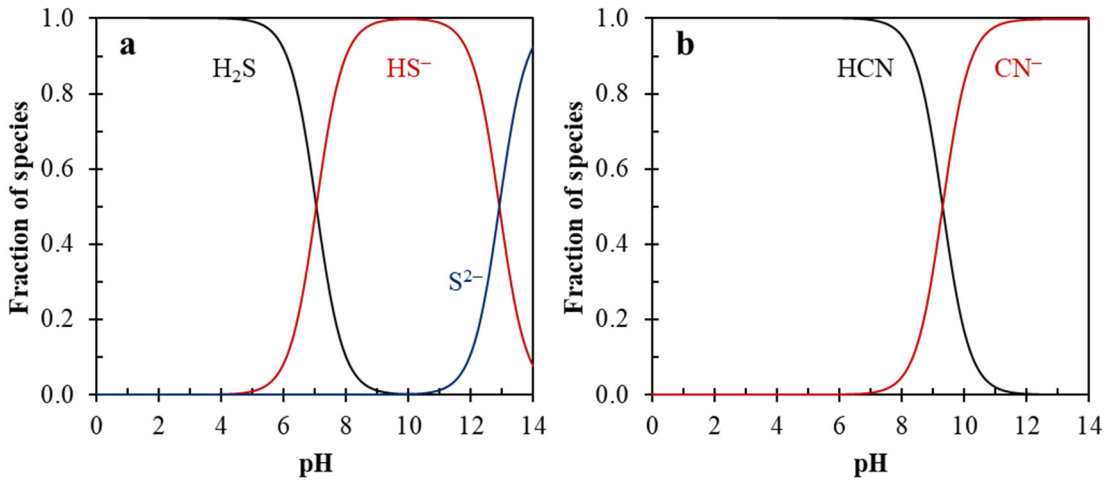

Figure 4. pH-dependent speciation of (**a**) sulfide (pK_{a1} = 7.1 and pK_{a2} = 12.9; $[S]_{tot}$ = 1 M) and (**b**) cyanide (pK_a = 9.3; $[CN]_{tot}$ = 1 M).

3. Alternative Options for Selective Flotation of Cu–Mo Bulk Concentrates

3.1. Molybdenite Depression

To replace the use of potentially toxic depressants such as NaHS and NaCN, there have been significant efforts to find suitable alternative depressants for molybdenite, for example, dextrin, lignosulfonate, carboxymethyl-based organic compounds, and humic acid. The summary of this section is present in Table 1.

Table 1. Summary of molybdenite depression.

Mo Depressant	Feed	Results	Features
Dextrin [22–26]	Natural MoS_2 [24], Cu ore (0.7–3.03% Cu, 0.011–0.14% Mo) [26].	✓ Mo recovery (R_{Mo}) decreased from 92% to 1.5% with 100 mg/L dextrin [24]. ✓ Recovery of Cu (R_{Cu}) and Mo (R_{Mo}) was 88.2% and 18.5%, respectively, with 200 g/t dextrin [26].	✓ In the presence of organic compound (e.g., iso-octane), the depressing efficiency of dextrin decreased [24]. ✓ Dextrin is effective in depressing MoS_2, but increases water recovery, causing the recovery of unwanted minerals [26].
Lignosulfonate [27–31]	Natural $CuFeS_2$ and MoS_2 [28].	✓ Single mineral-flotation tests showed that sodium-based lignosulfonates were effective in selectively depressing MoS_2 [28].	✓ Presence of Ca^{2+} introduced by calcium-based lignosulfonates and/or lime (pH adjuster) to the flotation system depressed not only MoS_2 but also $CuFeS_2$ [28].
O-carboxymethyl chitosan (O-CMC) [32,33]	Natural $CuFeS_2$ and MoS_2 [32].	✓ Selective depression of MoS_2 (R_{Mo} < 12%; R_{Cu} > 90%) was achieved using 150 ppm O-CMC with 20 ppm potassium isobutyl xanthate (KIBX) and 20 ppm methyl isobutyl carbinol (MIBC) at pH 5–9 [32].	✓ O-CMC could be adsorbed on both minerals but via different mechanisms; O-CMC was adsorbed on $CuFeS_2$ via weak physical interactions, while its adsorption on MoS_2 occurred via hydrophobic interactions [32,33].
Humic acid (HA) [34]	Natural $CuFeS_2$ and MoS_2 [34].	✓ Mixed-mineral flotation with 20 ppm HA resulted in >80% R_{Cu} and R_{Mo} ≈ 20% at pH 5–9 [34].	✓ Similar to O-CMC, the adsorption mechanisms of HA/$CuFeS_2$ and HA/MoS_2 were defined as electrostatic and hydrophobic interactions, respectively [34].
Carboxymethylcellulose (CMC) [35–37]	Natural MoS_2 [35].	✓ Two CMC polymers (i.e., HSHB and LSLB) were tested, and both were effective in depressing MoS_2; in SPW, R_{Mo} was 8% with 5 ppm HSHB and 2% with 5 ppm LSLB [35].	✓ CMCs act as both a Mo and a Cu depressant [36,37]. ✓ Depending on the type of ore, two approaches (i.e., (1) depressing MoS_2 with floating $CuFeS_2$ and (2) depressing $CuFeS_2$ with floating MoS_2) can be applicable [35–37].

3.1.1. Dextrin

Hernlund [22], for example, used dextrin as a Mo depressant. Dextrin is a water-soluble polysaccharide having the general formula of $(C_6H_{10}O_5)_n$, produced by the enzymatic hydrolysis

of starch [23,24]. The adsorption mechanism of dextrin molecules on the surface of molybdenite was proposed to occur via hydrophobic interaction [24,25]. As a result, the molybdenite surface is rendered hydrophilic, so its recovery decreased significantly from 92% to 1.5% when 100 mg/L dextrin was added [24]. A similar result was obtained by Jorjani et al. [26], who investigated the flotation behavior of porphyry copper ores containing Cu minerals (e.g., chalcopyrite and chalcocite), molybdenite, and aluminosilicates (e.g., albite, illite, kaolinite, muscovite, orthoclase, and vermiculite). This depressant could work well to decrease molybdenite recovery from around 50% to 15%; however, at a certain amount of added dextrin (i.e., 200 g/ton), it causes an increase in water content in froth products, resulting in the recovery of unwanted gangue minerals such as aluminosilicates by entrainment. In other words, it is recommended for froth products to be washed to obtain better products with low contents of undesired minerals [26]. Moreover, dextrin could not act as a Mo depressant in the presence of oily collectors, e.g., iso-octane (2,2,4-trimethylpentane, $(CH_3)_3CCH_2CH(CH_3)_2$), which is another disadvantage of the use of dextrin for Cu–Mo flotation [24].

3.1.2. Lignosulfonates

Lignosulfonates, a group of water-soluble and strong anionic polyelectrolytes typically obtained as a byproduct of wood processing for the extraction of cellulose [27,28], were first used for the separation of molybdenite and talc, both of which are hydrophobic in nature [29–31]. For molybdenite/talc separation, the reverse flotation of talc was proposed, where talc-bearing molybdenite ores are conditioned by lignosulfonate, with lime used as pH adjuster to increase the pH to around 11.5, resulting in the selective depression of molybdenite while talc is floated. In the case of chalcopyrite/molybdenite separation, however, the combination of lignosulfonate and lime depressed not only molybdenite but also chalcopyrite at pH ~11, making their separation impossible [28]. The floatability of chalcopyrite at the same pH but adjusted using KOH was unaffected by the presence of lignosulfonates. From these results, it can be concluded that Ca^{2+} has a strong effect on chalcopyrite depression, especially under alkaline conditions most likely due to the formation of $Ca(OH)_2$ on its surface. There are two possible mechanisms of how the formation of $Ca(OH)_2$ depresses the floatability of chalcopyrite: (1) $Ca(OH)_2$ is a hydrophilic compound, so it directly prevents the bubble attachment; and (2) the formation of $Ca(OH)_2$ changes the surface charge of chalcopyrite from negative to positive, making lignosulfonates (i.e., strong anionic polyelectrolytes) favorable to be adsorbed [27,28]. On the other hand, the floatability of molybdenite was strongly depressed by lignosulfonate in a wide pH range of 5–11, regardless of used pH adjusters (e.g., CaO, Na_2CO_3, and KOH). These results suggest that chalcopyrite/molybdenite separation could be achieved by using (not calcium-based) sodium sulfonates in the absence of Ca^{2+}. This means that lime, the most commonly used pH adjuster for depressing pyrite in bulk Cu/Mo flotation, is required to be replaced with other basic materials to eliminate the presence of Ca^{2+} in the pulp. Similar to the case of dextrin, lignosulfonates also lose their ability to depress molybdenite when the mineral surface is rendered hydrophobic by an oily collector such as dodecane ($CH_3(CH_2)_{10}CH_3$) prior to depressant adsorption [28].

3.1.3. Carboxymethyl-Based Organic Compounds and Humic Acid

O-carboxymethyl chitosan (O-CMC), a derivative of the second most abundant natural polysaccharide (i.e., chitosan), is nontoxic, biodegradable, cost-effective, and has better solubility in water compared to that of chitosan, which make it suitable for uses in a wide range of technologies. Yuan and coworkers [32,33] utilized O-CMC for the depression of molybdenite during Cu–Mo flotation. As shown in Figure 5a, the result of single-mineral flotation with 20 ppm potassium isobutyl xanthate (KIBX) showed that both minerals were highly recoverable (~97%) in the absence of O-CMC; however, with the addition of 150 ppm O-CMC, molybdenite was significantly depressed, and its recovery decreased to around 11%, whereas the floatability of chalcopyrite was not affected by O-CMC [32]. This selective depression of molybdenite was also achieved during the flotation of a Cu–Mo mixture in the presence of 150 ppm O-CMC (Figure 5b). The topographic atomic-force-microscopy (AFM) images

of chalcopyrite and molybdenite before and after treatment with O-CMC are illustrated in Figure 5c–f, showing that O-CMC created aggregates (100–200 nm diameter with ~2 nm height) that were only present on the surface of molybdenite. This result implies that O-CMC cannot be adsorbed on the chalcopyrite surface, but it is indeed possible according to their follow-up study [33]. Electrokinetic studies showed that the zeta potential of chalcopyrite treated with O-CMC notably decreased and was close to that of O-CMC macromolecules. In addition, X-ray photoelectron-spectroscopy (XPS) measurements of O-CMC-treated chalcopyrite indicated that apparent signatures of O-CMC were detected in the spectra of C 1s, N 1s, and O 1s. Although O-CMC could be adsorbed on the chalcopyrite surface, its adsorption is reversible due to the weak physical interactions (e.g., electrostatic interactions), which means that it could be mechanically desorbed. After washing O-CMC-treated chalcopyrite with Milli-Q water, in fact, the signals of adsorbed O-CMC disappeared in AFM and time-of-flight secondary ion-mass spectrometry (ToF-SIMS) imaging and diffused-reflectance infrared Fourier transform (DRIFT) spectroscopy [33]. However, O-CMC is adsorbed on the molybdenite basal planes via hydrophobic interactions that are more irreversible than those between O-CMC and chalcopyrite. Due to the different adsorption characteristics of O-CMC on chalcopyrite/molybdenite, selective depression of molybdenite could be achieved during Cu–Mo flotation. Yuan and coworkers [34] investigated the selective depression of humic acid (HA), a major organic constituent of soil and one of the most abundant naturally occurring organic macromolecules, for Cu–Mo flotation, and their results indicated that HA could selectively depress molybdenite by a similar adsorption mechanism as that of O-CMC; that is, the adsorption of HA on chalcopyrite and molybdenite takes place via electrostatic and hydrophobic interactions, respectively.

In the case of polymer adsorption on the mineral surface, electrolyte concentration and composition had considerable impact on adsorbed layer properties (e.g., thickness, coverage, and roughness) [35]. For example, Kor et al. [35] investigated the effects of electrolyte concentration and composition on the adsorption of two carboxymethylcellulose (CMC) polymers (high substitution, high blockiness (HSHB); low substitution, low blockiness (LSLB)) onto the molybdenite surface, and confirmed that higher ionic strength (2.76×10^{-2} M KCl) contributes to thicker layers with higher coverage compared to those observed in 10^{-2} M KCl (Table 2). Moreover, simulated process water (SPW), a complex electrolyte containing multivalent metal ions, further increases the thickness of adsorbed layers. As shown in Figure 6a, the flotation recovery of bare molybdenite in 10^{-2} M KCl electrolyte is around 92%, but the addition of 5 mg/L HSHB decreased Mo recovery to 30% in 10^{-2} M KCl, 14% in 2.76×10^{-2} M KCl, and 8% in SPW. Compared with HSHB, the depressing effect of LSLB for molybdenite is stronger, that is, the recovery of LSLB-treated molybdenite was 5% in in 10^{-2} M KCl, 4% in 2.76×10^{-2} M KCl, and 2% in SPW (Figure 6b), indicating that a thicker layer with higher coverage results in the better suppression of molybdenite floatability.

However, the floatability of chalcopyrite is also affected by HSHB and LSLB. In the absence of CMCs, the maximal recovery (R_{max}) of chalcopyrite is 91% ± 5%, whereas R_{max} is decreased to 66% ± 4% with 25 mg/L HSHB and 38% ± 2% with 25 mg/L LSLB [36]. According to Qui et al. [37], CMCs can be used for depressing chalcopyrite in Cu–Mo flotation separation. This means that the depressing ability of CMCs is not limited to molybdenite, that is, CMCs can play roles in depressing chalcopyrite and/or molybdenite, which is strongly dependent on operating conditions and ore compositions. Similarly, the problems with the use of organic polymers (e.g., starches and dextrins), widely used as a Pb depressant for Cu–Pb separation and as a pyrite depressant, are associated with the nonspecific depression of all sulfides when an excessive dosage is introduced [38]; thus, the flotation circuits using organic depressants need constant attention to avoid failure in sulfide separation.

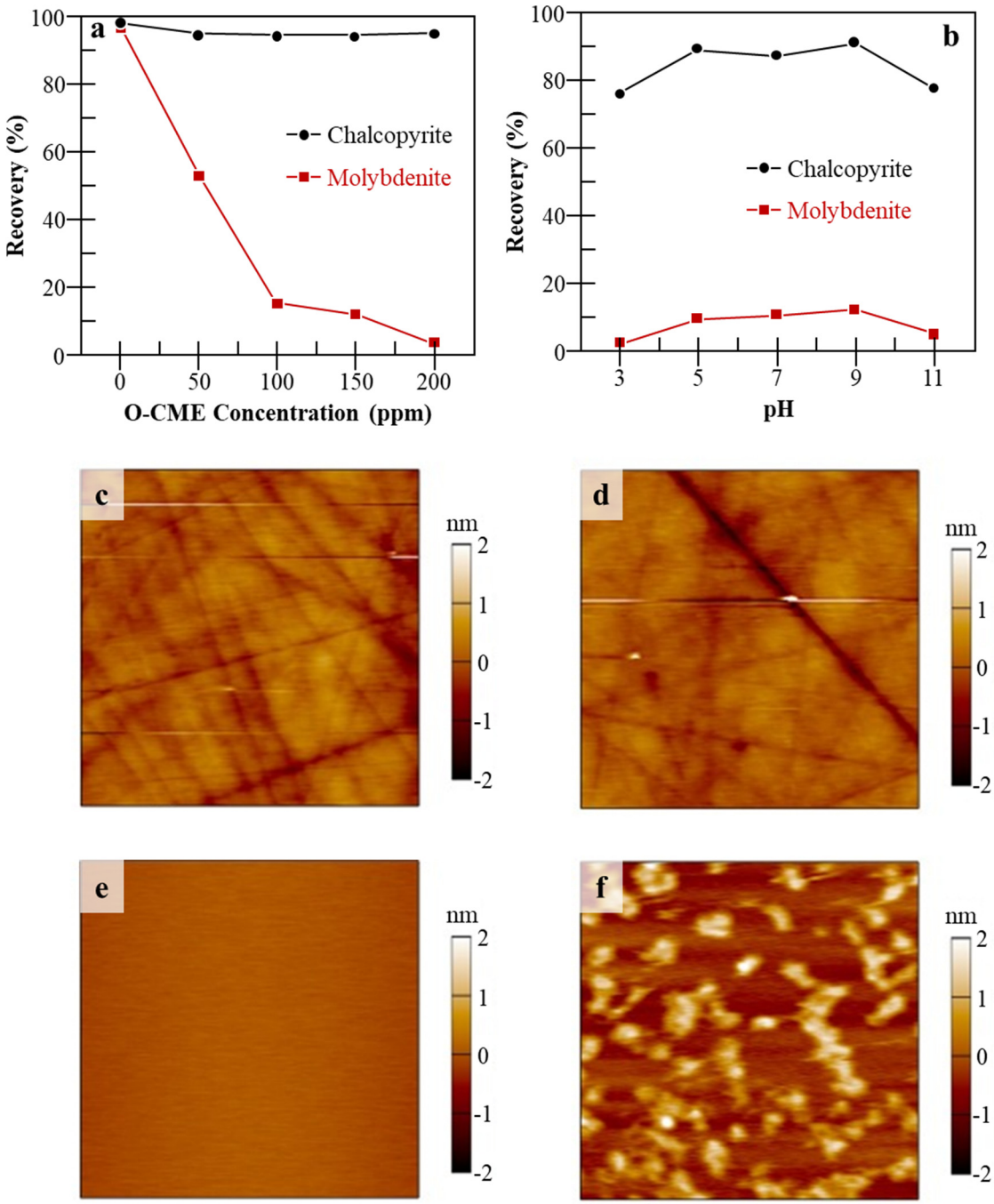

Figure 5. Effect of O-CMC on selective depression of molybdenite: (**a**) single-mineral flotation in 1 mM KCl solution with 20 ppm KIBX at pH 9 under various concentrations of O-CMC; (**b**) flotation of artificially mixed minerals (chalycopyrite:molybdenite = 1:1 by weight) in 1 mM KCl solution with 20 ppm KIBX and150 ppm O-CMC as function of pH, and atomic-force-microscopy (AFM) height profiles of (**c**) bare chalcopyrite, (**d**) chalcopyrite treated with 150 ppm O-CMC, (**e**) bare molybdenite, and (**f**) molybdenite treated with 150 ppm O-CMC (reprinted with permission from Yuan et al. [32], copyright (2019) Elsevier).

Table 2. Thickness and surface coverage (Γ) of adsorbed CMC (5 mg/L) at pH 9 on molybdenite (reprinted with permission from Kor et al. [35], copyright (2014) American Chemical Society). HSHB, high substitution, high blockiness; LSLB, low substitution, low blockiness; SPW, simulated process water.

Electrolyte	HSHB		LSLB	
	Thickness (nm)	Γ (%)	Thickness (nm)	Γ (%)
10^{-2} M KCl	1.1 ± 0.2	23	2.6 ± 0.2	100
2.76×10^{-2} M KCl	1.6 ± 0.6	95	4.0 ± 0.4	100
SPW *	2.7 ± 0.5	100	6.3 ± 0.4	100

* SPW consisted of 2.745 mM $CaSO_4$, 0.411 mM $Mg(NO_3)_2$, 4.653 mM Na_2SO_4, and 1.458 mM KCl.

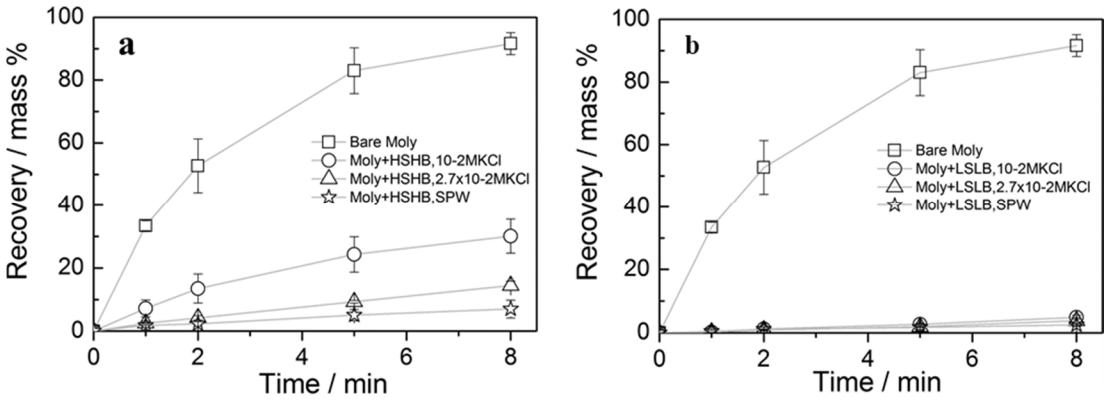

Figure 6. Single-mineral flotation of bare molybdenite and in presence of 5 mg/L CMC ((**a**) HSHB and (**b**) LSLB) at three studied electrolyte conditions: 10^{-2} M KCl, 2. 76×10^{-2} M KCl, and SPW, all at pH 9 (reprinted with permission from Kor et al. [35], copyright (2014) American Chemical Society).

3.2. Depression of Cu Minerals

As discussed in an earlier section, many molybdenite depressants could effectively improve the separation between Mo and Cu minerals. In the case of PCDs, however, the strategy of depressing chalcopyrite has been more commonly adopted than depressing molybdenite has, primarily due to mass-balance considerations [28], that is, the amount of molybdenite in PCDs is typically lower than that of Cu minerals, which makes the flotation process that recovers molybdenite by depressing chalcopyrite attractive. If the separation is done by the depression of molybdenite and the simultaneous flotation of chalcopyrite, it may cause the mechanical entrainment of molybdenite within a large volume of chalcopyrite concentrate [28], which lowers the grade of Cu concentrate, and leads to appreciable loss of molybdenite. Alternative depression techniques for chalcopyrite, including inorganic/organic depressants and oxidation treatments, are reviewed and summarized in Table 3.

Table 3. Summary of chalcopyrite depression.

Cu Depressant	Feed	Results	Features
Na_2SO_3 [39–45]	Natural $CuFeS_2$ and MoS_2 [44].	✓ With the addition of 0.1 M Na_2SO_3, $CuFeS_2$ floatability dramatically decreased to ≈ 0%, while >95% MoS_2 floated [44].	✓ Na_2SO_3 can also act as an activator for $CuFeS_2$, of which the surface is covered with ferric oxyhydroxide [45].
Seawater [46–58]	Natural $CuFeS_2$ and MoS_2 [49].	✓ Mixed-mineral flotation using artificial seawater at pH 10 resulted in lower recovery of both minerals (around 10–15%), but separation efficiency was greatly improved by using 416 mg/L emulsified kerosene (R_{Cu} > 70%, R_{Mo} ≈ 20%) [49].	✓ The adsorption of seawater precipitates (e.g., $Mg(OH)_2$ and $CaCO_3$) is the primary cause of both minerals' depression; however, emulsified oil limits its adsorption on MoS_2 [49].
Organic depressants (e.g., PGA [59], DMSA [60], DBT [61], chitosan [62–65], ATDT [66], and AHS [67])	Bulk Cu–Mo conc. [59], Cu–Mo ore [60], Cu–Mo rough conc. [61], natural $CuFeS_2$ and MoS_2 [62], $CuFeS_2$ and MoS_2 purified by flotation [66,67].	✓ All reviewed organic depressants were effective in depressing $CuFeS_2$, while they were negligible for MoS_2 floatability [59–62,66,67].	✓ S and/or N atoms in organic compounds have strong affinity with Cu atoms in $CuFeS_2$, making these organic depressants highly selective for $CuFeS_2$ [59–62,66,67].
Oxidation treatments (e.g., ozone (O_3) [68–73], plasma [74], H_2O_2 [13,75–77], and electrolysis [78]).	Bulk Cu–Mo conc. [69], natural $CuFeS_2$ and MoS_2 [13,74,75], mineral electrodes [78].	✓ After oxidation treatments, chalcopyrite is aggressively oxidized, resulting in a decrease in $CuFeS_2$ floatability due to the formation of hydrophilic oxidation products on its surface [13,69,74,75,78].	✓ MoS_2 was also oxidized, and on its surface, oxidation products (e.g., MoO_3) were formed; however, MoO_3 is highly soluble under alkaline conditions, so its effect on MoS_2 floatability becomes negligible under typical Cu–Mo flotation conditions (pH > 9) [13,74,75,78].

3.2.1. Inorganic Depressants

The xanthate-induced flotation of sulfide minerals is significantly influenced by pulp potential [39–42]. For example, the flotation of chalcopyrite using butyl xanthate shows that its recovery was lowered with decreasing Eh (Figure 7). At the Eh of −0.4 V, the addition of a collector had a negligible effect on the recovery of chalcopyrite, but was effective in the Eh range from −0.1 to 0.2 V due to the formation of a Cu(I)–xanthate complex (−0.1 to 0.0 V; Equation (10)) as well as dixanthogen (0.0 to 0.1 V; Equation (11)) [42].

$$CuX + FeS_2 + e^- \rightarrow CuFeS_2 + X^-, E^0 = -0.096\ V \quad (10)$$

$$X_2 + 2e^- \rightarrow 2X^-, E^0 = -0.009\ V \quad (11)$$

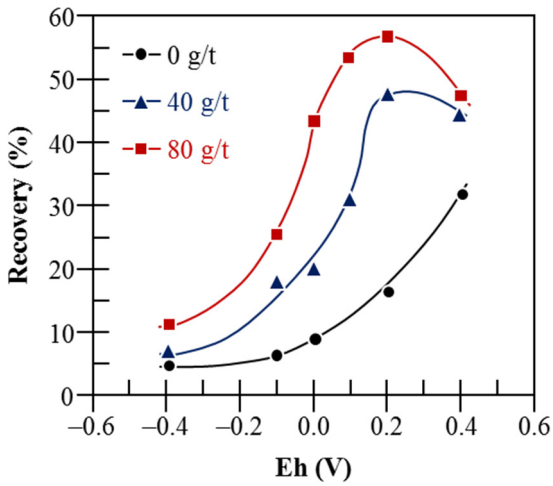

Figure 7. Recovery of chalcopyrite as function of Eh and butyl xanthate addition at pH 8.1 (reprinted with permission from Grano et al. [39], copyright (1990) Elsevier).

At an Eh greater than 0.2 V, however, the recovery of chalcopyrite started decreasing because of the decomposition of the Cu(I)–xanthate complex (Equation (12)), making the mineral surface less hydrophobic [43].

$$2HCuO_2^- + X_2 + 6H^+ + 4e^- \rightarrow 2CuX + 4H_2O,\ E^0 = -1.402\ V \quad (12)$$

On the basis of Eh dependence on chalcopyrite flotation, Miki et al. [44] used Na_2SO_3 as a depressant that provided the reducing conditions where the floatability of chalcopyrite decreased. The flotation results using a TMD solution (mixture of TX15216 (alkyl mercaptan), MX-7017 (modified thionocarbamate), and diesel oil), and methyl isobutyl carbinol (MIBC) as collector and frother, respectively, indicated that molybdenite was recovered by more than 95%, while the recovery of chalcopyrite was almost 0% when conditioned with 0.1 M Na_2SO_3 at pH 10.8 for 1 h (Figure 8a). XPS spectra of chalcopyrite treated with Na_2SO_3 showed that various hydrophilic species (i.e., CuO, $Cu(OH)_2$, FeOOH, and $Fe_2(SO_4)_3$) were formed on its surface. Miki and coworkers [44] proposed the mechanism on the formation of hydrophilic compounds that occurs via a series of reactions; that is, reductive dissolution of chalcopyrite by Na_2SO_3 (Equation (13)), oxidative dissolution of Cu_2S (Equation (14)), and hydrolysis/precipitation of Cu^{2+} and Fe^{3+} (Equations (15)–(18)).

$$2CuFeS_2 + 6Cu^{2+} + 3SO_3^{2-} + 6OH^- \rightarrow 4Cu_2S + 2Fe^{3+} + 3SO_4^{2-} + 3H_2O \quad (13)$$

$$Cu_2S \rightarrow 2Cu^{2+} + S + 4e^- \quad (14)$$

$$Cu^{2+} + H_2O \rightarrow CuO + 2H^+ \quad (15)$$

$$Cu^{2+} + 2H_2O \rightarrow Cu(OH)_2 + 2H^+ \quad (16)$$

$$Fe^{3+} + 2H_2O \rightarrow FeOOH + 3H^+ \quad (17)$$

$$2Fe^{3+} + 3SO_4^{2-} \rightarrow Fe_2(SO_4)_3 \quad (18)$$

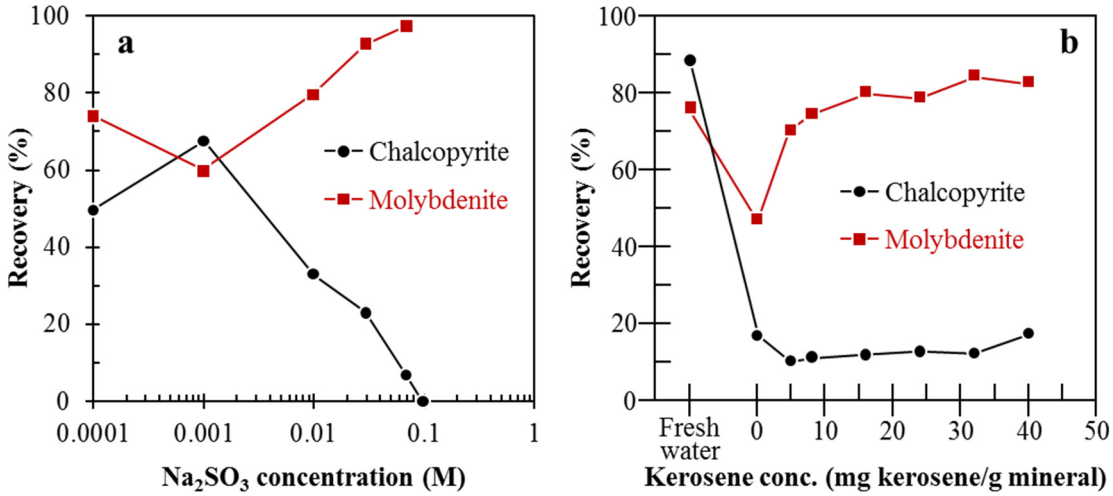

Figure 8. Recovery of chalcopyrite and molybdenite with varying concentrations of (**a**) Na_2SO_3 in TMD solution (mixture of TX15216 (alkyl mercaptan), MX-7017 (modified thionocarbamate), and diesel oil) [43] and (**b**) kerosene in $MgCl_2$ solution (reprinted with permission from Hirajima et al. [54], copyright (2016) Elsevier).

Meanwhile, the change in molybdenite surface after Na_2SO_3 treatment was almost negligible, indicating that the molybdenite surface remained hydrophobic. These results support the potential of Na_2SO_3 as a Cu depressant for Cu–Mo flotation separation. However, Na_2SO_3 does not always depress the floatability of chalcopyrite, but it can act as an activator depending on the state of the chalcopyrite surface. In the case of chalcopyrite, of which the surface is significantly covered with ferric oxyhydroxide, for example, the floatability of chalcopyrite is depressed to entrainment level (i.e., <10%) due to the presence of the hydrophilic nature of ferric oxyhydroxide on its surface. Meanwhile, the depressing effect of adsorbed ferric species is diminished when Na_2SO_3 is introduced because ferric species are reductively dissolved by SO_3^{2-} (Equations (19) and (20)), resulting in the exposure of iron-deficient chalcopyrite [45]. Therefore, the use of Na_2SO_3 as a Cu depressant should be carefully designed to avoid the failure of Cu–Mo separation.

$$SO_4^{2-} + H_2O + 2e^- \rightarrow SO_3^{2-} + 2OH^-, E^0 = -0.93\ V \quad (19)$$

$$Fe(OH)_3 + e^- \rightarrow Fe(OH)_2 + OH^-, E^0 = -0.56\ V \quad (20)$$

In arid and semiarid regions where the supply of fresh water is limited, the use of seawater in mineral-processing plants is a sustainable option. However, seawater, a concentrated solution of NaCl (around 0.6 M) with various secondary ions (e.g., 0.41 g/L Ca^{2+}, 1.28 g/L Mg^{2+}, 2.71 g/L SO_4^{2-}, and 0.11 g/L HCO_3^-), significantly changes the flotation behavior of molybdenite [46–49]. For example, the floatability of chalcopyrite is not affected by types of water sources (i.e., fresh and sea water) in the pH range of 7.5–11.5, but molybdenite is dramatically depressed in seawater when pH is higher than 9.5–10.0 [47,50–52]. This indicates that a significant amount of molybdenite is lost during rougher and cleaner flotation if the pulp pH is adjusted to 10–12 by using lime for depressing pyrite [47]. The primary detrimental effect on molybdenite floatability is due to the adsorption of magnesium hydroxy complexes ($Mg(OH)^+_{(aq)}$) and magnesium hydroxide precipitates ($Mg(OH)_{2(s)}$), which start forming at a pH above around 9.5 [50]. Qui et al. [53] analyzed the surface of molybdenite conditioned in seawater at pH 11 by using scanning electron microscopy (SEM), auger electron spectroscopy (AES), XPS, and ToF-SIMS, and confirmed that colloidal $Mg(OH)_2$ and crystallized $CaCO_3$ were deposited on the molybdenite surface. Meanwhile, Hirajima et al. [54] reported that $Mg(OH)_2$ depressed not only molybdenite but also chalcopyrite at pH > 9. Similarly, Nagaraj and Farinato [55] also reported that both molybdenite and chalcopyrite floatability was decreased in Mg^{2+}-containing solution at

pH > 9.5 although the former was more strongly affected than the latter was. These indicate that seawater does not always show identical impact on Cu recovery, which changes depending on the type of used reagents and ore compositions [49]. In the case that both Cu and Mo were depressed by $Mg(OH)_2$, Hirajima and coworkers [54] proposed the utilization of kerosene emulsion for the flotation separation of chalcopyrite and molybdenite in a 0.01 M $MgCl_2$ solution (equivalent to about 243 mg/L Mg^{2+}). As shown in Figure 8b, the recoveries of chalcopyrite and molybdenite in 0.01 M $MgCl_2$ solution at pH 11 decreased from 90% to 18% and from 75% to 50%, respectively; however, molybdenite recovery was selectively improved with the addition of kerosene emulsion. Comparing the dynamic-force-microscopy (DFM) images of molybdenite surfaces conditioned in 0.01 M $MgCl_2$ at pH 11 with and without emulsified kerosene, the coverage of precipitate on molybdenite surface was apparently lower when kerosene was conditioned together. This is most likely because kerosene is a nonpolar oily collector that has strong affinity with molybdenite; thus, it is preferably adsorbed on the molybdenite surface, which limits the attachment of $Mg(OH)_2$. The study of Suyantara et al. [49], a follow-up study of Hirajima et al. [54], reported that kerosene emulsion could also be used for improving Cu–Mo flotation separation in artificial seawater. In the case that only molybdenite is depressed in seawater under alkaline conditions (i.e., pH 10–12), three options can be proposed: (1) the use of dispersants (e.g., sodium hexametaphosphate (SHMP)) to disperse seawater precipitates adsorbed on molybdenite surface [56,57]; (2) the removal of problematic ions (e.g., Ca^{2+} and Mg^{2+}) using Na_2CO_3 and CaO prior to rougher/cleaner flotation [58]; and (3) the operation of rougher/cleaner flotation at a pH lower than 9.5, where Ca^{2+}/Mg^{2+} precipitations are limited, with alternative pyrite depressants that can act at pH < 9.5 [47].

3.2.2. Organic Depressants

Along with the investigation on inorganic depressants, there have been many studies on organic depressants; for example, pseudo-glycolythiourea acid (PGA) [59], 2,3-disulfanylbutanedioic acid (DMSA) [60], disodium bis (carboxymethyl) trithiocarbonate (DBT) [61], chitosan [62], 4-amino-3-thioxo-3,4-dihydro-1,2,4-triazin-5(2H)-one (ATDT) [66], and acetic acid-[(hydrazinylthioxomethyl)thio]-sodium (AHS) [67]. Chen and coworkers [59] used PGA (Figure 9a) and investigated its effect on Cu–Mo separation. Under the optimized conditions, Mo recovery reached around 90% with a grade of 26% (original grade in feed = 0.4%) via one rougher (375 g/t Na_2SiO_3, 4000 g/t PGA, and 200 g/t kerosene), one scavenger (500 g/t PGA and 200 g/t kerosene), and two cleaners (62 g/t Na_2SiO_3, 1000 g/t, and 66 g/t kerosene), where Na_2SiO_3, PGA, and kerosene were used as a dispersant, Cu depressant, and Mo collector, respectively. Meanwhile, the recovery of Cu was around 0.7%, and its grade decreased from 18% (Cu grade in feed) to 10% (Cu grade in concentrate), indicating that PGA could be used as a Cu depressant in Cu–Mo flotation. To understand the mechanism of how PGA selectively depresses chalcopyrite, Chen et al. [59] conducted PGA adsorption tests with single minerals of chalcopyrite and molybdenite, and the results suggested that PGA was adsorbed on both minerals' surfaces, but the adsorption capacity of chalcopyrite was much larger compared to that of molybdenite. Infrared (IR) analyses of minerals after PGA adsorption tests indicated that the IR spectrum of PGA-adsorbed chalcopyrite was significantly changed with the appearance of new peaks (e.g., —COOH and —CS— of PGA), the disappearance of chalcopyrite peaks, and the great shift of SO_4^{2-} peaks. These changes in IR signatures were most likely caused by the chemisorption between S atoms in PGA, the most reactive site based on its largest electron density of highest occupied molecular orbital (HOMO), and Cu atoms on the chalcopyrite surface. On the other hand, the IR spectrum of molybdenite showed only small shifts of absorption peaks less than 3 cm^{-1}, which indicated that PGA is physically adsorbed on the surface of molybdenite. Even in the presence of butyl xanthate (BX), the most common collector for sulfide flotation, PGA could be adsorbed on chalcopyrite and molybdenite surfaces. The adsorption capacity of BX on both minerals' surfaces decreased as PGA concentration increased, which means that BX adsorption was limited due to the competitive adsorption between PGA and BX on chalcopyrite and molybdenite surfaces. Moreover, PGA has strong

reducibility that can reduce dixanthogen molecules formed on chalcopyrite and molybdenite surfaces via the electrochemical reaction of BX. Fermi energies (E_F) of PGA, molybdenite, and chalcopyrite are −3.936, −4.138, and −5.433 eV, respectively. The direction of electron transition is always from a high- to a low-energy level; thus, PGA preferably gave the electrons to chalcopyrite than to molybdenite when the two minerals coexisted.

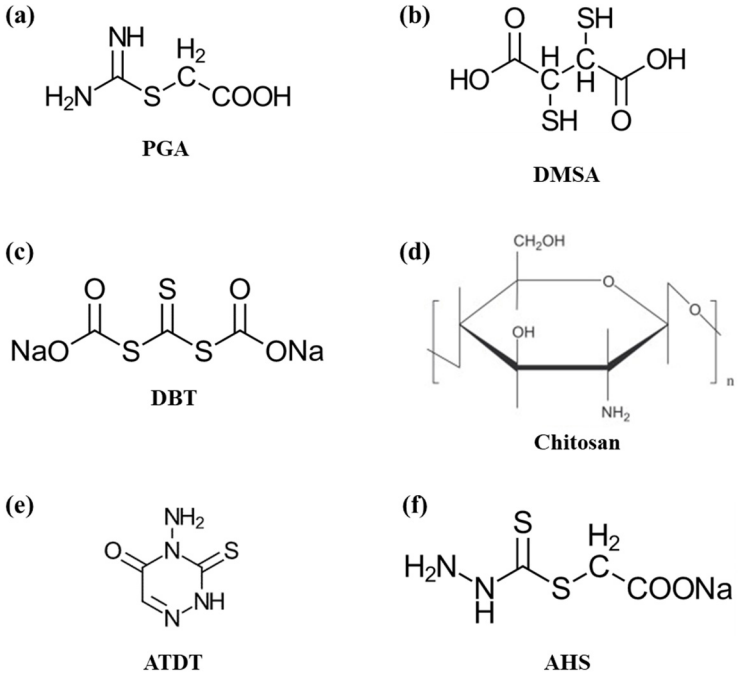

Figure 9. Molecular structure of organic depressants: (**a**) pseudo-glycolythiourea acid (PGA), (**b**) 2,3-disulfanylbutanedioic acid (DMSA), (**c**) disodium bis (carboxymethyl) trithiocarbonate (DBT), (**d**) chitosan (reprinted with permission from Crini and Badot [65], copyright (2008) Elsevier), (**e**) 4-amino-3-thioxo-3,4-dihydro-1,2,4-triazin-5(2H)-one (ATDT), and (**f**) acetic acid-[(hydrazinylthioxomethyl)thio]-sodium (AHS).

A novel and selective depressant named DMSA was first used in the flotation of Cu–Mo sulfides by Li and coworkers [60]. As illustrated in Figure 9b, DMSA contains two carboxyl and two sulfhydryl groups. Adsorption tests showed that DMSA can be adsorbed more intensively on chalcopyrite than molybdenite can; that is, the adsorption capacities of DMSA on chalcopyrite and molybdenite were 0.29 and 0.05 mg/g, respectively. According to the calculation based on frontier-molecular-orbital (FMO) theory, the largest electron density of HOMO is located on two S atoms, both of which actively interact with minerals. Additionally, it is interesting to note that the Fermi energies of DMSA, molybdenite, and chalcopyrite are −5.573, −4.353, and −6.110 eV, respectively, which indicate that the electron transfer between DMSA and chalcopyrite, an essential process for the adsorption of organic with a strong reducibility, occurs more easily than that between DMSA and molybdenite, consistent with the adsorption results. A similar result was obtained from the study of Yin et al. [61] who used DBT as a depressant (Figure 9c). The IR spectrum of molybdenite after DBT treatment showed that the characteristic bands of DBT were not observed; however, the IR spectrum of DBT-treated chalcopyrite showed the appearance of new peaks of C=S stretching, C—O stretching, CH_2 wagging, CH_2 scissoring, and C—C stretching, not observed in the IR spectrum of chalcopyrite without DBT treatment, indicating that DBT was notably adsorbed on the chalcopyrite surface. The DBT-treated chalcopyrite was further analyzed by XPS, and the C 1s and S 2p spectra also proved the presence of DBT on its surface. The S $2p_{3/2}$ peaks of DBT adsorbed on the chalcopyrite surface were shifted to higher binding energies than those of DBT, while the binding energies of Cu $2p_{3/2}$ and Cu $2p_{1/2}$ were shifted to lower positions after DBT was adsorbed. From these results, Yin and coworkers [61] concluded that S atoms in DBT

(i.e., the electron donor) might interact with the Cu atoms in chalcopyrite (i.e., the electron acceptor). Due to the selective and strong affinity of DMSA and DBT with chalcopyrite, those organic compounds could be successfully used as a Cu depressant in Cu–Mo flotation.

As such, organic depressants that contain S atom(s) as a constituent in their molecules, such as PGA, DMSA, and DBT, have the strong ability to selectively depress chalcopyrite in Cu–Mo concentrates. Another attempt of using chitosan (Figure 9d) has also been made for the same purpose [62–64]. Chitosan, a natural biodegradable and nontoxic polyaminosaccharide, contains an amino functional group (—NH_2) known to have strong affinity with Cu^{2+}, which implies that it can specifically interact with Cu-bearing minerals. Li and coworkers [62] used chitosan as a Cu depressant in Cu–Mo flotation. According to the result of single-mineral flotation, chitosan depressed both chalcopyrite and molybdenite, but it was effective in selectively depressing chalcopyrite when both minerals existed together in the pulp. This result could be explained by the competitive adsorption of chitosan between the two minerals, proved by adsorption isotherm tests, which showed that the adsorption density of chitosan on chalcopyrite was greater than that on molybdenite. As a result, chitosan could succeed in the selective flotation of molybdenite from Cu–Mo concentrates, that is, the recoveries of molybdenite and chalcopyrite in the froth product were around 70% and 24%, respectively. Furthermore, organic compounds that contained both amine- and thione-functional groups, such as ATDT (Figure 9e) and AHS (Figure 9f), were reported to be effective in depressing chalcopyrite due to bidentate coordination to $Cu^{I/II}$ via S and N atoms to form a stable five-membered chelating ring (Figure 10) [66,67]. The selectivity index (SI) of Mo/Cu in the absence of a depressant was around 1.44, but considerably improved to 2.98 with ATDT and to 5.77 with AHS.

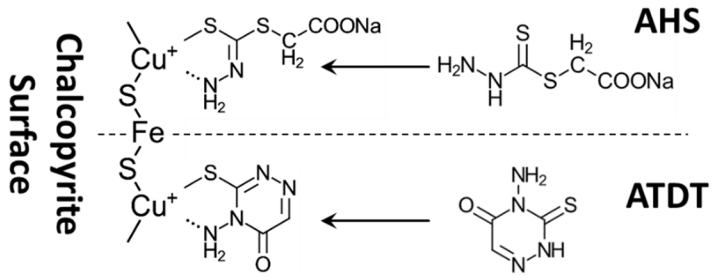

Figure 10. Proposed adsorption models of AHS and ATDT on chalcopyrite surface.

3.3. Oxidation Treatments for Depressing Cu Minerals

3.3.1. Ozone Oxidation

In the early 1990s, the application of ozone (O_3) for the depression of Cu minerals (e.g., chalcopyrite and chalcocite) and the selective recovery of molybdenite from Cu–Mo bulk concentrates was studied [68,69]. Ozone, a strong oxidant, as illustrated in Equations (21) and (22), is widely used for water treatment due to its exceptional ability to oxidize organic compounds and to disinfect bacteria [70,71].

$$O_3 + 6H^+ + 6e^- \rightarrow 3H_2O,\ E^0 = 1.51\ V \quad (21)$$

$$O_3 + 2H^+ + 2e^- \rightarrow O_2 + H_2O,\ E^0 = 2.07\ V \quad (22)$$

Moreover, the decomposition of ozone in water produces hydroxyl radicals ($HO^\bullet$) (Equation (23)), which are among the most reactive free radicals and among the strongest oxidants (Equation (24)) [71,72].

$$O_3 + H_2O \rightarrow 2HO^\bullet + O_2 \quad (23)$$

$$HO^\bullet + H^+ + e^- \rightarrow H_2O,\ E^0 = 2.33\ V \quad (24)$$

In the typical flotation process of Cu–Mo ores (Figure 2), the flotation separation of Cu and Mo from Cu–Mo bulk concentrates is achieved by using NaHS, which desorbs the adsorbed xanthate on the chalcopyrite surface, that is, chalcopyrite becomes unrecoverable as a froth product while molybdenite is selectively floated and recovered. Although xanthates are known as weak collectors of molybdenite, it can also be adsorbed on the surface of molybdenite [73]. However, the molybdenite surface is naturally hydrophobic, so even in the absence of xanthate on its surface, molybdenite is still floatable with nonpolar oily collectors (e.g., diesel oil and kerosene), which makes the desorption of xanthate by NaHS strongly affect the floatability of chalcopyrite rather than that of molybdenite. Similar to NaHS, the utilization of ozone, having strong potential to oxidize organic compounds, can improve Cu–Mo flotation separation by destroying xanthate adsorbed onto the mineral surface. Ye et al. [69] utilized ozone as a conditioning process for Cu–Mo separation, and reported that ozone conditioning oxidized all tested minerals (e.g., chalcocite, chalcopyrite, and molybdenite), leading to their floatability lowering. However, Cu minerals are more sensitive to ozone compared to molybdenite, so the selective depression of Cu minerals is possible by employing ozone-based oxidation treatment. For example, a flotation circuit that consists of a rougher flotation with ozone conditioning for 2 min, followed by a cleaner flotation after 3 min of ozone treatment of low-grade Cu–Mo concentrate (0.25% Mo), can produce a Mo concentrate of which grade and recovery are 26% and 82.5%, respectively [69]. After rougher flotation, 10.5% of molybdenite still remained in rougher tailing, which was further conditioned with ozone for 1 min, followed by scavenger flotation. The distributions of Mo in scavenger concentrate and cleaner tailings are 9.4% and 7.0%, respectively, indicating that overall Mo recovery would be expected to reach 98.9% when they were reintroduced to the process (denoted as dotted lines in Figure 11).

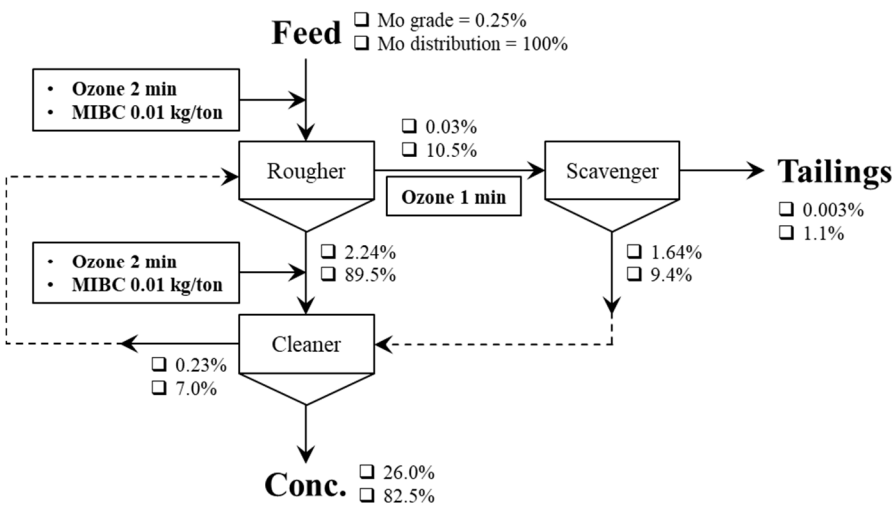

Figure 11. Flowsheet for selective flotation of molybdenite from Cu–Mo concentrates using three-stage ozone conditioning. Dotted lines represent possible recycle streams (reprinted with permission from Ye et al. [69], copyright (1990) Springer Nature).

3.3.2. Plasma Oxidation

Similarly, Hirajima et al. [74] examined oxidation treatment using plasma as a conditioning process for the selective flotation of chalcopyrite and molybdenite. After 10 min treatment of chalcopyrite with plasma at 10 W, AFM images showed that the chalcopyrite surface became rough (3.979 nm) compared to the one without plasma treatment (1.280 nm), and there was no significant effect of washing on the change in surface roughness (Figure 12). In the case of molybdenite, its surface roughness increased from 3.797 to 5.176 nm after plasma treatment (10 W) for 10 min, but it became smooth when washing followed; that is, the washing of plasma-treated molybdenite for 30, 60, and 120 min decreased its surface roughness to 4.263, 3.484, and 3.289 nm, respectively. The presence of reaction products on the

surfaces of chalcopyrite and molybdenite after plasma treatment significantly affected their floatability. As shown in Figure 13a, the recovery of untreated chalcopyrite and molybdenite was around 90%, but dramatically decreased to 10–30% after plasma treatment. Washing following could improve the floatability of molybdenite treated with plasma, whereas chalcopyrite recovery was kept constant regardless of washing. To clarify the flotation behaviors of chalcopyrite and molybdenite with plasma treatment followed by washing, Hirajima et al. [74] conducted XPS analysis of plasma-treated minerals with various washing times. The result of XPS analysis of plasma-treated molybdenite showed that it was covered with molybdenum(VI) oxide (MoO_3); however, the peaks of MoO_3 in Mo 3d and O 1s spectra were lowered after washing. In the case of plasma-treated chalcopyrite, its surface was covered with goethite (FeOOH) and iron(III) sulfate ($Fe_2(SO_4)_3$), both of which are oxidation products of chalcopyrite having hydrophilic properties. After washing, the peaks of iron(III) sulfate disappeared, while goethite still remained on the surface of chalcopyrite. This is the reason why the floatability of plasma-treated chalcopyrite did not increase even after washing for 120 min. Washing cannot improve molybdenite floatability when both minerals are treated together by plasma. This might be due to iron ions (e.g., Fe^{2+} and/or Fe^{3+}) being released from chalcopyrite that are precipitated on the surface of not only chalcopyrite but also molybdenite, reducing the hydrophobicity of both minerals. To overcome this limited recovery of molybdenite, Hirajima and coworkers [74] investigated the addition of kerosene, a commonly used reagent for Mo flotation. As a result of the addition of 25 μL emulsified kerosene, molybdenite recovery increased from around 40% to 80%, while it had a negligible effect on chalcopyrite recovery, increasing from 20% to 30%.

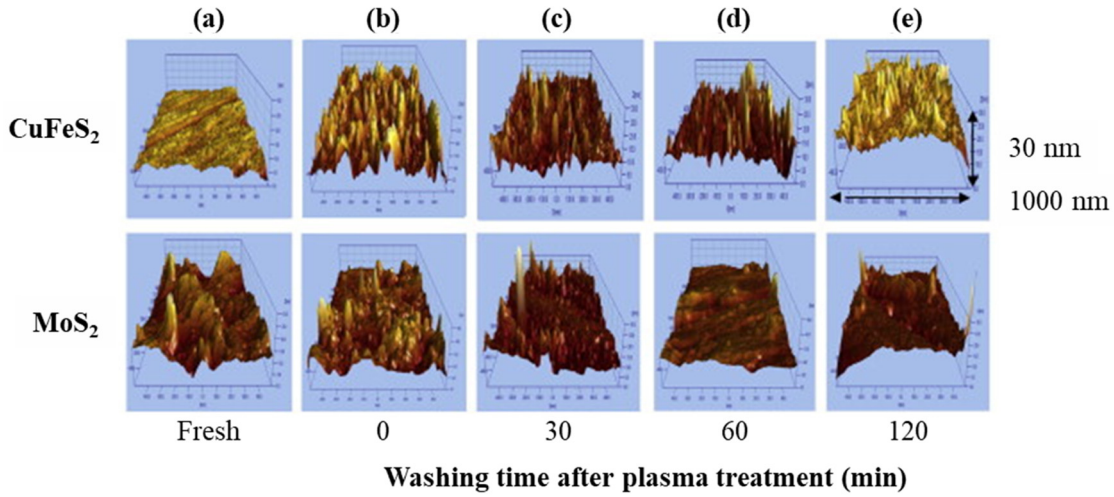

Figure 12. AFM images of chalcopyrite and molybdenite: (**a**) untreated samples and one treated with plasma at 10 W for 10 min followed by washing by pH 9 solution for (**b**) 0, (**c**) 30, (**d**) 60, and (**e**) 120 min (reprinted with permission from Hirajima et al. [74], copyright (2014) Elsevier).

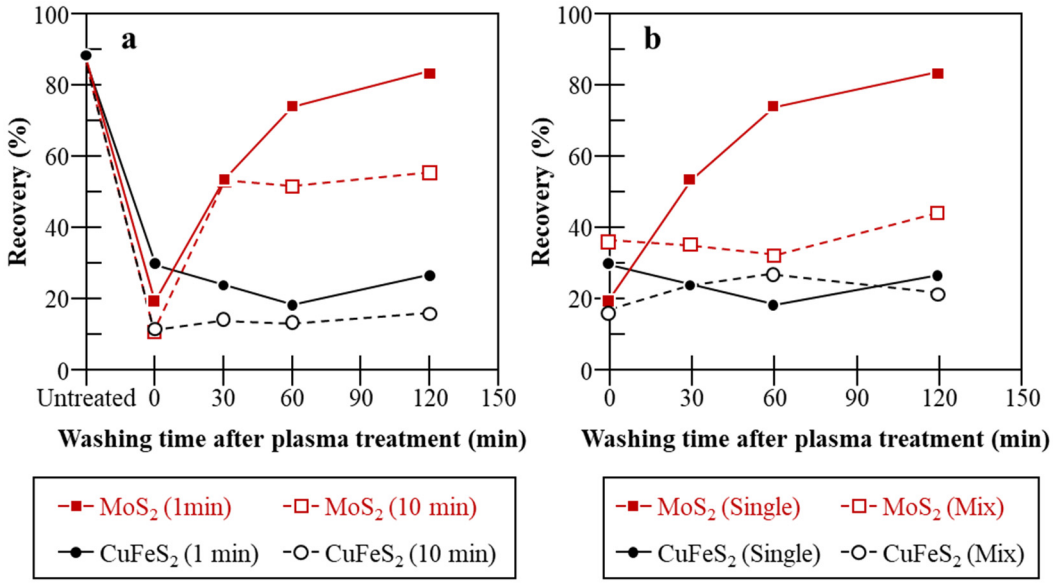

Figure 13. Flotation recovery of chalcopyrite and molybdenite treated (**a**) with and without 10 W plasma for 1 or 10 min followed by washing (single system), and (**b**) with 10 W plasma for 1 min followed by washing (single and mixed system) (reprinted with permission from Hirajima et al. [74], copyright (2014) Elsevier).

3.3.3. H_2O_2 Oxidation

Although plasma treatment for Cu–Mo ores prior to flotation was effective in improving the separation of chalcopyrite and molybdenite, its application on an industrial scale remains difficult to realize [75]. Because of this limitation, Hirajima and coworkers [13] examined another oxidation process using hydrogen peroxide (H_2O_2), which acts as an oxidant under acidic conditions (Equation (25)), but behaves as a reductant under alkaline conditions (Equation (26)).

$$H_2O_2 + 2H^+ + 2e^- \rightarrow 2H_2O, E^0 = 1.78\ V \quad (25)$$

$$H_2O_2 \rightarrow 2H^+ + O_2 + 2e^-, E^0 = -0.68\ V \quad (26)$$

Moreover, H_2O_2 can produce hydroxyl and hydroperoxyl radicals ($HO^\bullet$ and $HOO^\bullet$, respectively) acting as powerful oxidizing agents in the presence of iron ions (e.g., Fe^{2+} and Fe^{3+}) via Fenton (Fe^{2+}/H_2O_2) and Fenton-like (Fe^{3+}/H_2O_2) reactions, as shown in the following equations:

$$Fe^{2+} + H_2O_2 \rightarrow Fe^{3+} + HO^\bullet + OH^-, \quad (27)$$

$$Fe^{3+} + H_2O_2 \rightarrow Fe^{2+} + HOO^\bullet + H^+. \quad (28)$$

After 10 min treatment of chalcopyrite using 0.1% H_2O_2, the floatability of chalcopyrite decreased from 85% to 19%, most likely due to the formation of hydrophilic oxidation products (e.g., CuO, $Cu(OH)_2$, FeOOH, and $Fe_2(SO_4)_3$) on the chalcopyrite surface. Meanwhile, the floatability of molybdenite was not affected by H_2O_2 treatment (the recoveries of untreated and H_2O_2-treated molybdenite were 73% and 79%, respectively) because the oxidation products of molybdenite (e.g., MoO_2 and MoO_3) are soluble under alkaline conditions. Hirajima et al. [13] also compared the effectiveness of oxidation treatments using ozone and H_2O_2 on Cu–Mo flotation separation, and it was confirmed that H_2O_2 treatment showed better separation efficiency compared to that of ozone treatment because ozone reduced the recovery of not only chalcopyrite (from 85% to 28%), but also molybdenite (from 73% to 53%). Although effective, the application of H_2O_2 treatment to Cu–Mo bulk concentrates with high pulp density (around 50%) has some drawbacks compared to the NaHS method: (1) molybdenite

recovery by H_2O_2-based flotation is lower than that of conventional flotation process using NaHS; (2) it requires a prolonged treatment of around 4.5 h to effectively depress the floatability of chalcopyrite, while 10 min is enough for the NaHS method; and (3) it uses a high concentration of H_2O_2 (i.e., 2%), which makes H_2O_2-based flotation costly [75]. To overcome these limitations of H_2O_2 oxidation treatment, Suyantara and coworkers [75] investigated the simultaneous use of H_2O_2 and $FeSO_4$, which can stimulate a Fenton-like reaction. In an alkaline solution, $FeSO_4$ releases Fe^{2+}, which is then transformed into iron oxyhydroxide (goethite, α-FeOOH; lepidocrocite, γ-FeOOH) and/or ferrihydrite, where a Fenton-like reaction occurs in the presence of H_2O_2 as shown in the following equations [76]:

$$\equiv Fe^{III}\text{–}OH + H_2O_2 \rightarrow (H_2O_2)_s \tag{29}$$

$$(H_2O_2)_s \rightarrow \equiv Fe^{II} + H_2O + HOO^{\bullet} \tag{30}$$

$$\equiv Fe^{II} + H_2O_2 \rightarrow \equiv Fe^{III}\text{–}OH + HO^{\bullet} \tag{31}$$

$$HOO^{\bullet} \rightarrow H^+ + O_2^{\bullet -} \tag{32}$$

$$\equiv Fe^{III}\text{–}OH + HOO^{\bullet}/O_2^{\bullet -} \rightarrow \equiv Fe^{II} + H_2O/OH^- + O_2. \tag{33}$$

According to Li et al. [77], who evaluated the decomposition rate of H_2O_2 in the absence and presence of FeOOH, it was confirmed that the addition of FeOOH significantly enhanced H_2O_2 decomposition compared to the one without FeOOH. Suyantara et al. [75], who used H_2O_2 with $FeSO_4$ for the oxidation treatment of Cu–Mo bulk concentrates prior to flotation, confirmed that the addition of $FeSO_4$ could reduce the amount of added H_2O_2 from 2.0% to 0.5% and treatment time from 4.5 h to 5 min. Due to these positive effects of $FeSO_4$ addition to H_2O_2 oxidation treatment, the process of using H_2O_2 and $FeSO_4$ is predicted to reduce operating costs, that is, the costs for NaHS, H_2O_2, and $H_2O_2/FeSO_4$ methods were calculated to approximately 20, 100, and 15 USD/t, respectively [75].

3.3.4. Electrolysis Oxidation

The electrical resistivities of chalcopyrite and molybdenite are 234 Ω and 1.2–1.5 MΩ, respectively, which means that chalcopyrite is more electrochemically active than molybdenite is [78]. From the difference in the minerals' electrical resistivity, Miki et al. [78] attempted to apply electrolysis, a technique that applies a fixed potential in which mineral undergoes oxidation process(es) to selectively render the chalcopyrite surface hydrophilic. Anodic polarization results at an applied potential of 1.2 V showed that a high current density of chalcopyrite electrodes (around 0.4 mA/m^2) was observed, indicating that the oxidation of chalcopyrite was actively progressed, as shown in the following equation:

$$CuFeS_2 + 8H_2O \rightarrow Cu^{2+} + Fe^{2+} + 2SO_4^{2-} + 16H^+ + 16e^-. \tag{34}$$

On the other hand, the current density of molybdenite electrodes was around 0.05–0.15 mA/m^2, substantially lower compared to that of chalcopyrite. This most likely resulted from the high resistivity of molybdenite, which makes it difficult to be oxidized. After treating chalcopyrite and molybdenite electrodes by electrolysis oxidation at 1.2 V for 800 s, the contact angle of chalcopyrite changed from 71.7° to 42.4°, whereas there was almost no effect on the contact angle of molybdenite, changing from 68.6° to 67.0°. The contact-angle results indicate that electrolysis treatment could selectively convert the wettability of chalcopyrite from hydrophobic to hydrophilic. Although flotation tests of electrolysis-treated chalcopyrite/molybdenite were not conducted, electrolysis oxidation is in a promising state as pretreatment for improving the selective flotation of molybdenite from Cu–Mo concentrates.

3.4. Microencapsulation Techniques for Depressing Cu Minerals

As discussed in Section 3.3.4, chalcopyrite and molybdenite have different electrical resistivities, which means that the depression techniques involved in electrochemical processes have the potential to

be applied to Cu–Mo flotation separation. For example, the authors studied carrier microencapsulation (CME), a technique that creates metal-oxyhydroxide coatings on the surfaces of semiconducting minerals such as pyrite and arsenopyrite (FeAsS) [79–84]. In CME, metal ions (e.g., Al^{3+}, Fe^{3+}, Si^{4+}, and Ti^{4+}) and the organic carrier (e.g., catechol, 1,2-dihydroxybenzene, and $C_6H_4(OH)_2$) are used, and they produce various forms of metal–catecholate complexes (e.g., $[Al(cat)_n]^{3-2n}$, $[Fe(cat)_n]^{3-2n}$, $[Si(cat)_3]^{2-}$ and $[Ti(cat)_3]^{2-}$, where n is 1–3). These complexes undergo oxidative decomposition only on the surface of semiconducting minerals such as pyrite and arsenopyrite (FeAsS), and metal ions released from the complexes are then precipitated as metal oxyhydroxides (Figure 14). Similar to CME, other microencapsulation techniques involved in electrochemical process(es) are most likely able to selectively form hydrophilic coatings on the surface of chalcopyrite having relatively low electrical resistivity, while the molybdenite surface is not covered with the coatings because it is hard for electrochemical reactions to occur on its surface. Although there is no study on this topic, it is of importance to develop environmentally friendly processes for Cu–Mo flotation separation.

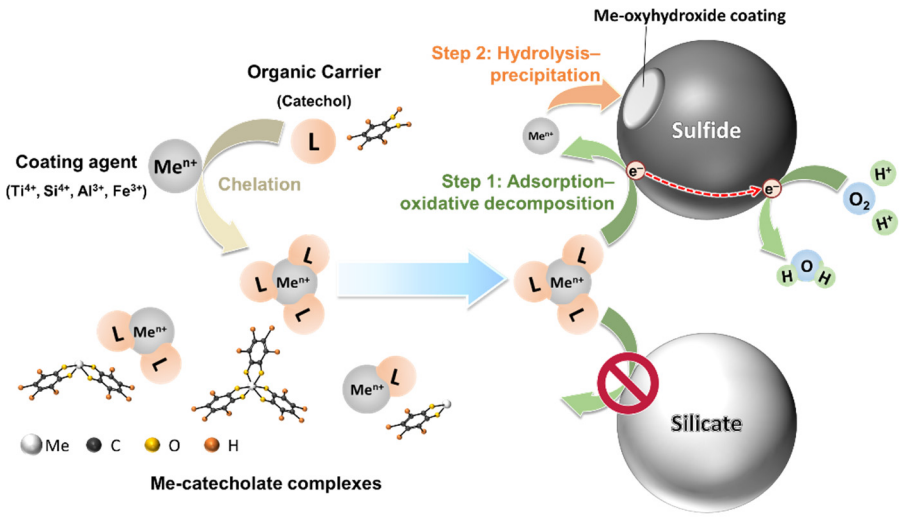

Figure 14. Schematic diagram of carrier microencapsulation (reprinted with permission from Park et al. [83], copyright (2019) Elsevier).

4. Summary

Porphyry copper deposits are one of the most important sources of copper and molybdenum. The separation/recovery of copper and molybdenum from these deposits is typically processed by a flotation series, that is, bulk flotation to remove gangue minerals and produce Cu–Mo concentrates that are then processed by Cu–Mo flotation to separate them. In Cu–Mo flotation, various types of Cu depressants (e.g., NaHS, Na_2S, Nokes reagent, and NaCN) have been adopted for selective depression of Cu minerals. However, these reagents are potentially dangerous due to the possibility of emitting toxic and deadly gases, such as H_2S and HCN, when operating conditions are not properly controlled. To avoid accidents caused by the use of conventional Cu depressants, there are many studies on the utilization of environmentally friendly depressants for molybdenite or chalcopyrite, and oxidation treatments for chalcopyrite.

For the depression of molybdenite, various organic compounds, such as dextrin, lignosulfonate, O-carboxymethyl chitosan, carboxymethyl cellulose, and humic acid, were adopted. Molybdenite is well-known to have strong hydrophobicity, so those organic compounds are favorably and selectively adsorbed on the molybdenite surface via hydrophobic interactions. The utilization of Mo depressants is effective for the separation of Cu and Mo minerals, but there is a serious drawback, lowering the purity of froth products. This is because the content of molybdenite in PCDs is substantially lower than that of chalcopyrite, so the strategy of recovering chalcopyrite with the depression of molybdenite can cause the mechanical entrainment of molybdenite within a large volume of Cu concentrate, which

lowers the grade of Cu concentrate and leads to appreciable loss of molybdenite. Another option for Cu–Mo flotation separation is to depress Cu minerals while recovering molybdenite. For this, alternative organic/inorganic depressants were extensively examined. Moreover, oxidation treatments using ozone, plasma, H_2O_2, and electrolysis to destroy adsorbed xanthate and/or to create hydrophilic coatings on the surface of chalcopyrite were studied. The obtained results are promising for Cu–Mo separation; however, there still remain important topics on the optimization and scaling-up of the process that are necessary for the application of newly developed depression techniques to actual Cu–Mo flotation separation.

Author Contributions: Conceptualization, I.P., S.H., S.J., M.I., and N.H.; writing—original-draft preparation, I.P.; writing—review and editing, I.P., S.H., S.J., M.I., and N.H.; visualization, I.P. All authors have read and agreed to the published version of the manuscript.

Funding: This research was financially supported by Japan Oil, Gas, and Metals National Corporation (JOGMEC).

Conflicts of Interest: The authors declare no conflict of interest.

References

1. John, D.A.; Ayuso, R.A.; Barton, M.D.; Blakely, R.J.; Bodnar, R.J.; Dilles, J.H.; Gray, F.; Graybeal, F.T.; Mars, J.C.; McPhee, D.K.; et al. *Porphyry Copper Deposit Model: Chapter B of Mineral Deposit Models for Resource Assessment*; Scientific Investigations Report 2010–5070–B; US Geological Survey: Menlo Park, CA, USA, 2010; 169p.
2. John, D.A.; Taylor, R.D. By-products of porphyry copper and molybdenum deposits. *Rev. Econ. Geol.* **2016**, *18*, 137–164.
3. Lee, C.-T.A.; Tang, M. How to make porphyry copper deposits. *Earth Planet. Sci. Lett.* **2020**, *529*, 115868. [CrossRef]
4. Seedorff, E.; Dilles, J.H.; Proffett, J.M., Jr.; Einaudi, M.T.; Zurcher, L.; Stavast, W.J.A.; Johnson, D.A.; Barton, M.D. Porphyry deposits: Characteristics and origin of hypogene features. *Econ. Geol.* **2005**, *100*, 251–298.
5. Sinclair, W.D. Porphyry deposits. In *Mineral Deposits of Canada: A Synthesis of Major Deposit-Types, District Metallogeny, the Evolution of Geological Provinces, and Exploration Methods, Geological Association of Canada, Mineral Deposits Division*; Goodfellow, W.D., Ed.; Special Publication: London, UK, 2007; Volume 5, pp. 223–243.
6. Bulatovic, S.M. 12–Flotation of Copper Sulfide Ores. In *Handbook of Flotation Reagents*; Bulatovic, S.M., Ed.; Elsevier: Amsterdam, The Netherlands, 2007; pp. 235–293, ISBN 978-0-444-53029-5.
7. Amelunxen, P.; Schmitz, C.; Hill, L.; Goodweiler, N.; Andres, J. Molybdenum. In *SME Mineral Processing & Extractive Metallurgy Handbook*; Dunne, R.C., Komar Kawatra, S., Young, C.A., Eds.; Society for Mining, Metallurgy & Exploration (SME): Littleton, CO, USA, 2019; Volume 2, pp. 1891–1916.
8. Liu, G.; Lu, Y.; Zhong, H.; Cao, Z.; Xu, Z. A novel approach for preferential flotation recovery of molybdenite from a porphyry copper-molybdenum ore. *Miner. Eng.* **2012**, *36*, 37–44. [CrossRef]
9. Peterson, J.A.; Saran, M.S.; Wisnouskas, J.S. Differential Flotation Reagent for Molybdenum Separation. U.S. Patent No. 4,575,419, 11 March 1986.
10. Yin, Z.; Sun, W.; Hu, Y.; Zhai, J.; Qingjun, G. Evaluation of the replacement of NaCN with depressant mixtures in the separation of copper-molybdenum sulphide ore by flotation. *Sep. Purif. Technol.* **2017**, *173*, 9–16. [CrossRef]
11. Sutherland, K.L.; Wark, I.W. *Principles of Flotation*, 2nd ed.; Australasian Inst. Mining & Metallurgy: Melbourne, Australia, 1955.
12. Mu, Y.; Peng, Y.; Lauten, R.A. The depression of pyrite in selective flotation by different reagent systems—A literature review. *Miner. Eng.* **2016**, *96–97*, 143–156. [CrossRef]
13. Hirajima, T.; Miki, H.; Suyantara, G.P.W.; Matsuoka, H.; Elmahdy, A.M.; Sasaki, K.; Imaizumi, Y.; Kuroiwa, S. Selective flotation of chalcopyrite and molybdenite with H_2O_2 oxidation. *Miner. Eng.* **2017**, *100*, 83–92. [CrossRef]
14. Napier-Munn, T.; Wills, B.A. *Wills' Mineral Processing Technology: An Introduction to the Practical Aspects of Ore Treatment and Mineral Recovery*, 7th ed.; Butterworth-Heinemann: Oxford, UK, 2006.

15. Zhao, Q.; Liu, W.; Wei, D.; Wang, W.; Cui, B.; Liu, W. Effect of copper ions on the flotation separation of chalcopyrite and molybdenite using sodium sulfide as a depressant. *Miner. Eng.* **2018**, *115*, 44–52. [CrossRef]
16. Guo, B.; Peng, Y.; Espinosa-Gomez, R. Cyanide chemistry and its effect on mineral flotation. *Miner. Eng.* **2014**, *66–68*, 25–32. [CrossRef]
17. Sinozaki, H.; Hara, R.; Mitsukuri, S. The vapour pressures of hydrogen cyanide. *Bull. Chem. Soc. Jpn.* **1926**, *1*, 59–61. [CrossRef]
18. Stull, D.R. Vapor pressure of pure substances. Organic and inorganic compounds. *Ind. Eng. Chem.* **1947**, *39*, 517–540. [CrossRef]
19. Milby, T.H.; Baselt, R.C. Hydrogen sulfide poisoning: Clarification of some controversial issues. *Am. J. Ind. Med.* **1999**, *35*, 192–195. [CrossRef]
20. National Research Council. *Acute Exposure Guideline Levels for Selected Airborne Chemicals: Volume 2*; The National Academies Press: Washington, DC, USA, 2002. [CrossRef]
21. Johnston, A.; Meadows, D.G.; Cappuccitti, F. Copper mineral processing. In *SME Mineral Processing & Extractive Metallurgy Handbook*; Dunne, R.C., Komar Kawatra, S., Young, C.A., Eds.; Society for Mining, Metallurgy & Exploration (SME): Littleton, CO, USA, 2019; Volume 2, pp. 1615–1642.
22. Hernlund, R.W. Extraction of molybdenite from copper flotation products. *Q. J. Colo. Sch. Mines* **1961**, *56*, 177–196.
23. Blanco, M.; Coello, J.; Iturriaga, H.; Maspoch, S.; González Bañó, R. On-line monitoring of starch enzymatic hydrolysis by near-infrared spectroscopy. *Analyst* **2000**, *125*, 749–752. [CrossRef]
24. Wie, J.M.; Fuerstenau, D.W. The effect of dextrin on surface properties and the flotation of molybdenite. *Int. J. Miner. Process.* **1974**, *1*, 17–32. [CrossRef]
25. Beaussart, A.; Mierczynska-Vasilev, A.; Beattie, D.A. Adsorption of dextrin on hydrophobic minerals. *Langmuir* **2009**, *25*, 9913–9921. [CrossRef]
26. Jorjani, E.; Barkhordari, H.R.; Tayebi Khorami, M.; Fazeli, A. Effects of aluminosilicate minerals on copper-molybdenum flotation from Sarcheshmeh porphyry ores. *Miner. Eng.* **2011**, *24*, 754–759. [CrossRef]
27. Ansari, A.; Pawlik, M. Floatability of chalcopyrite and molybdenite in the presence of lignosulfonates. Part I. Adsorption studies. *Miner. Eng.* **2007**, *20*, 600–608. [CrossRef]
28. Ansari, A.; Pawlik, M. Floatability of chalcopyrite and molybdenite in the presence of lignosulfonates. Part II. Hallimond tube flotation. *Miner. Eng.* **2007**, *20*, 609–616. [CrossRef]
29. Buza, T.B.; Hiscox, T.O.; Kuhn, M.C. Use of lignin sulphonate as moly depressant boosts recovery at Twin Buttes. *Eng. Min. J.* **1975**, *176*, 87–91.
30. Mathieu, G.; Bruce, R. Getting the talc out of molybdenite ores. *Can. Min. J.* **1974**, *95*, 75–77.
31. Yuan, D.; Cadien, K.; Liu, Q.; Zeng, H. Separation of talc and molybdenite: Challenges and opportunities. *Miner. Eng.* **2019**, *143*, 105923. [CrossRef]
32. Yuan, D.; Cadien, K.; Liu, Q.; Zeng, H. Flotation separation of Cu-Mo sulfides by O-Carboxymethyl chitosan. *Miner. Eng.* **2019**, *134*, 202–205. [CrossRef]
33. Yuan, D.; Cadien, K.; Liu, Q.; Zeng, H. Adsorption characteristics and mechanisms of O-Carboxymethyl chitosan on chalcopyrite and molybdenite. *J. Colloid Interface Sci.* **2019**, *552*, 659–670. [CrossRef] [PubMed]
34. Yuan, D.; Cadien, K.; Liu, Q.; Zeng, H. Selective separation of copper-molybdenum sulfides using humic acids. *Miner. Eng.* **2019**, *133*, 43–46. [CrossRef]
35. Kor, M.; Korczyk, P.M.; Addai-Mensah, J.; Krasowska, M.; Beattie, D.A. Carboxymethylcellulose adsorption on molybdenite: The effect of electrolyte composition on adsorption, bubble–surface collisions, and flotation. *Langmuir* **2014**, *30*, 11975–11984. [CrossRef]
36. Mierczynska-Vasilev, A.; Beattie, D.A. Adsorption of tailored carboxymethyl cellulose polymers on talc and chalcopyrite: Correlation between coverage, wettability, and flotation. *Miner. Eng.* **2010**, *23*, 985–993. [CrossRef]
37. Qui, X.; Yang, H.; Chen, G.; Luo, W. An Alternative Depressant of Chalcopyrite in Cu–Mo Differential Flotation and Its Interaction Mechanism. *Minerals* **2019**, *9*, 1.
38. Bulatovic, S.M. Use of organic polymers in the flotation of polymetallic ores: A review. *Miner. Eng.* **1999**, *12*, 341–354. [CrossRef]

39. Grano, S.; Ralston, J.; Smart, R.S.C. Influence of electrochemical environment on the flotation behavior of Mt. Isa copper and lead-zinc ore. *Int. J. Miner. Process.* **1990**, *30*, 69–97. [CrossRef]
40. Heyes, G.W.; Trahar, W.J. The natural flotability of chalcopyrite. *Int. J. Miner. Process.* **1977**, *4*, 317–344. [CrossRef]
41. Ralston, J. Eh and its consequences in sulphide mineral flotation. *Miner. Eng.* **1991**, *4*, 859–878. [CrossRef]
42. Richardson, P.E.; Walker, G.W. The flotation of chalcocite, bornite, chalcopyrite, and pyrite in an electrochemical-flotation cell. In Proceedings of the XV International Mineral Processing Congress, Cannes, France, 2–9 June 1985; pp. 198–210.
43. Guy, P.J.; Trahar, W.J. The effects of oxidation and mineral interaction on sulphide flotation. In *Flotation of Sulphide Minerals*; Forrsberg, K.S.E., Ed.; Elsevier: Amsterdam, The Netherlands, 1985; pp. 91–110.
44. Miki, H.; Hirajima, T.; Muta, Y.; Suyantara, G.P.W.; Sasaki, K. Effect of sodium sulfite on floatability of chalcopyrite and molybdenite. *Minerals* **2018**, *8*, 172. [CrossRef]
45. Grano, S.R.; Sollaart, M.; Skinner, W.; Prestidge, C.A.; Ralston, J. Surface modification in the chalcopyrite-sulphite ion system. I. collectorless flotation, XPS and dissolution study. *Int. J. Miner. Process.* **1997**, *50*, 1–26. [CrossRef]
46. Castro, S.; Laskowski, J.S. Froth flotation in saline water. *KONA Powder Part. J.* **2011**, *29*, 4–15. [CrossRef]
47. Castro, S. Challenges in flotation of Cu–Co sulfide ores in sea water. In *The First International Symposium on Water in Mineral Processing*; Drelich, J., Ed.; Society for Mining, Metallurgy & Exploration (SME): Littleton, CO, USA, 2012; pp. 29–40.
48. Laskowski, J.S.; Castro, S.; Ramos, O. Effect of seawater main components on frothability in the flotation of Cu-Mo sulfide ore. *Physicochem. Probl. Miner. Process.* **2013**, *50*, 17–29.
49. Suyantara, G.P.W.; Hirajima, T.; Miki, H.; Sasaki, K. Floatability of molybdenite and chalcopyrite in artificial seawater. *Miner. Eng.* **2018**, *115*, 117–130. [CrossRef]
50. Castro, S.; Rioseco, P.; Laskowski, J.S. Depression of molybdenite in sea water. In Proceedings of the XXVI International Mineral Processing Congress, New Delhi, India, 24–28 September 2012; pp. 737–752.
51. Laskowski, J.S.; Castro, S. Flotation in concentrated electrolyte solutions. *Int. J. Miner. Process.* **2015**, *144*, 50–55. [CrossRef]
52. Ramos, O.; Castro, S.; Laskowski, J.S. Copper-molybdenum ores flotation in sea water: Floatability and frothability. *Miner. Eng.* **2013**, *53*, 108–112. [CrossRef]
53. Qui, Z.; Liu, G.; Liu, Q.; Zhong, H. Understanding the roles of high salinity in inhibiting the molybdenite flotation. *Colloids Surf. A Physicochem. Eng. Asp.* **2016**, *509*, 123–129.
54. Hirajima, T.; Suyantara, G.P.W.; Ichikawa, O.; Elmahdy, A.M.; Miki, H.; Sasaki, K. Effect of Mg^{2+} and Ca^{2+} as divalent seawater cations on the floatability of molybdenite and chalcopyrite. *Miner. Eng.* **2016**, *96–97*, 83–93. [CrossRef]
55. Nagaraj, D.R.; Farinato, R. Chemical factor effects in saline and hypersaline waters in the flotation of Cu and Cu-Mo ores. In Proceedings of the XXVII International Mineral Processing Congress, Santiago, Chile, 20–24 October 2014; pp. 20–24.
56. Li, W.; Li, Y.; Wei, Z.; Xiao, Q.; Song, S. Fundamental Studies of SHMP in Reducing Negative Effects of Divalent Ions on Molybdenite Flotation. *Minerals* **2018**, *8*, 404. [CrossRef]
57. Rebolledo, E.; Laskowski, J.S.; Gutierrez, L.; Castro, S. Use of dispersants in flotation of molybdenite in seawater. *Miner. Eng.* **2017**, *100*, 71–74. [CrossRef]
58. Jeldres, R.I.; Arancibia-Bravo, M.P.; Reyes, A.; Aguirre, C.E.; Cortes, L.; Cisternas, L.A. The impact of seawater with calcium and magnesium removal for the flotation of copper-molybdenum sulphide ores. *Miner. Eng.* **2017**, *109*, 10–13. [CrossRef]
59. Chen, J.; Lan, L.; Liao, X. Depression effect of pseudo glycolythiourea acid in flotation separation of copper–molybdenum. *Trans. Nonferrous Met. Soc. China* **2013**, *23*, 824–831. [CrossRef]
60. Li, M.; Wei, D.; Shen, Y.; Liu, W.; Gao, S.; Liang, G. Selective depression effect in flotation separation of copper-molybdenum sulfides using 2,3-disulfanylbutanedioic acid. *Trans. Nonferrous Met. Soc. China* **2015**, *25*, 3126–3132. [CrossRef]

61. Yin, Z.; Sun, X.; Hu, Y.; Guan, Q.; Zhang, C.; Gao, Y.; Zhai, J. Depressing behaviors and mechanism of disodium bis (carboxymethyl) trithiocarbonate on separation of chalcopyrite and molybdenite. *Trans. Nonferrous Met. Soc. China* **2017**, *27*, 883–890. [CrossRef]
62. Li, M.; Wei, D.; Liu, Q.; Liu, W.; Zheng, J.; Sun, H. Flotation separation of copper-molybdenum sulfides using chitosan as a selective depressant. *Miner. Eng.* **2015**, *83*, 217–222. [CrossRef]
63. Yin, Z.; Sun, W.; Hu, Y.; Zhang, C.; Guan, Q.; Zhang, C. Separation of molybdenite from chalcopyrite in the presence of novel depressant 4-amino-3-thioxo-3,4-dihydro-1,2,4-triazin-5(2H)-one. *Minerals* **2017**, *7*, 146.
64. Yin, Z.; Sen, W.; Hu, Y.; Zhang, C.; Guan, Q.; Liu, R.; Chen, P.; Tian, M. Utilization of acetic acid-[(hydrazinylthioxomethyl)thio]-sodium as a novel selective depressant for chalcopyrite in the flotation separation of molybdenite. *Sep. Purif. Technol.* **2017**, *179*, 248–256. [CrossRef]
65. Huang, P.; Cao, M.; Liu, Q. Using chitosan as a selective depressant in the differential flotation Cu-Pb sulfides. *Int. J. Miner. Process.* **2012**, *106–109*, 8–15. [CrossRef]
66. Huang, P.; Cao, M.; Liu, Q. Adsorption of chitosan on chalcopyrite and galena from aqueous suspensions. *Colloids Surf. A Physicochem. Eng. Asp.* **2012**, *409*, 167–175. [CrossRef]
67. Crini, G.; Badot, P.-M. Application of chitosan, a natural aminopolysaccharide, for dye removal from aqueous solutions by adsorption processes using batch studies: A review of recent literature. *Prog. Polym. Sci.* **2008**, *33*, 399–447. [CrossRef]
68. Miller, J.D.; Ye, Y.; Jang, W.-H. Molybdenite Flotation from Copper Sulfide/Molybdenite Containing Materials by Ozone Conditioning. U.S. Patent No. 5,068,028, 26 November 1991.
69. Ye, Y.; Jang, W.H.; Yalamanchili, M.R.; Miller, J.D. Molybdenite flotation from copper/molybdenum concentrates by ozone conditioning. *Miner. Metall. Process.* **1990**, *7*, 173–179. [CrossRef]
70. Da Silva, L.M.; Jardim, W.F. Trends and strategies of ozone application in environmental problems. *Quim. Nova* **2006**, *29*, 310–317. [CrossRef]
71. Kasprzyk-Hordern, B.; Ziółek, M.; Nawrocki, J. Catalytic ozonation and methods of enhancing molecular ozone reactions in water treatment. *Appl. Catal. B Environ.* **2003**, *46*, 639–669. [CrossRef]
72. Huang, C.P.; Dong, C.; Tang, Z. Advanced chemical oxidation: Its present role and potential future in hazardous waste treatment. *Waste Manag.* **1993**, *13*, 361–377. [CrossRef]
73. Castro, S.; Lopez-Valdivieso, A.; Laskowski, J.S. Review of the flotation of molybdenite. Part I: Surface properties and floatability. *Int. J. Miner. Process.* **2016**, *148*, 48–58. [CrossRef]
74. Hirajima, T.; Mori, M.; Ichikawa, O.; Sasaki, K.; Miki, H.; Farahat, M.; Sawada, M. Selective flotation of chalcopyrite and molybdenite with plasma. *Miner. Eng.* **2014**, *66–68*, 102–111. [CrossRef]
75. Suyantara, G.P.W.; Hirajima, T.; Miki, H.; Sasaki, K.; Yamane, M.; Takida, E.; Kuroiwa, S.; Imaizumi, Y. Selective flotation of chalcopyrite and molybdenite using H_2O_2 oxidation method with the addition of ferrous sulfate. *Miner. Eng.* **2018**, *122*, 312–326. [CrossRef]
76. Lin, S.-S.; Gurol, M.D. Catalytic decomposition of hydrogen peroxide on iron oxide: Kinetics, mechanism, and implications. *Environ. Sci. Technol.* **1998**, *32*, 1417–1423. [CrossRef]
77. Li, X.; Huang, Y.; Li, C.; Shen, J.; Deng, Y. Degradation of pCNB by Fenton like process using α-FeOOH. *Chem. Eng. J.* **2015**, *260*, 28–36. [CrossRef]
78. Miki, H.; Matsuoka, H.; Hirajima, T.; Suyantara, G.P.W.; Sasaki, K. Electrolysis oxidation of chalcopyrite and molybdenite for selective flotation. *Mater. Trans.* **2017**, *58*, 761–767. [CrossRef]
79. Jha, R.K.T.; Satur, J.; Hiroyoshi, N.; Ito, M.; Tsunekawa, M. Carrier-microencapsulation using Si-catechol complex for suppressing pyrite floatability. *Miner. Eng.* **2008**, *21*, 889–893. [CrossRef]
80. Li, X.; Hiroyoshi, N.; Tabelin, C.B.; Naruwa, K.; Harada, C.; Ito, M. Suppressive effects of ferric-catecholate complexes on pyrite oxidation. *Chemosphere* **2019**, *214*, 70–78. [CrossRef]
81. Park, I.; Tabelin, C.B.; Magaribuchi, K.; Seno, K.; Ito, M.; Hiroyoshi, N. Suppression of the release of arsenic from arsenopyrite by carrier-microencapsulation using Ti-catechol complex. *J. Hazard. Mater.* **2018**, *344*, 322–332. [CrossRef]
82. Park, I.; Tabelin, C.B.; Seno, K.; Jeon, S.; Ito, M.; Hiroyoshi, N. Simultaneous suppression of acid mine drainage and arsenic release by carrier-microencapsulation using aluminum-catecholate complexes. *Chemosphere* **2018**, *205*, 414–425. [CrossRef] [PubMed]

83. Park, I.; Tabelin, C.B.; Jeon, S.; Li, X.; Seno, K.; Ito, M.; Hiroyoshi, N. A review of recent strategies for acid mine drainage prevention and mine tailings recycling. *Chemosphere* **2019**, *219*, 588–606. [CrossRef]
84. Park, I.; Tabelin, C.B.; Seno, K.; Jeon, S.; Inano, H.; Ito, M.; Hiroyoshi, N. Carrier-microencapsulation of arsenopyrite using Al-catecholate complex: Nature of oxidation products, effects on anodic and cathodic reactions, and coating stability under simulated weathering conditions. *Heliyon* **2020**, *6*, e03189. [CrossRef]